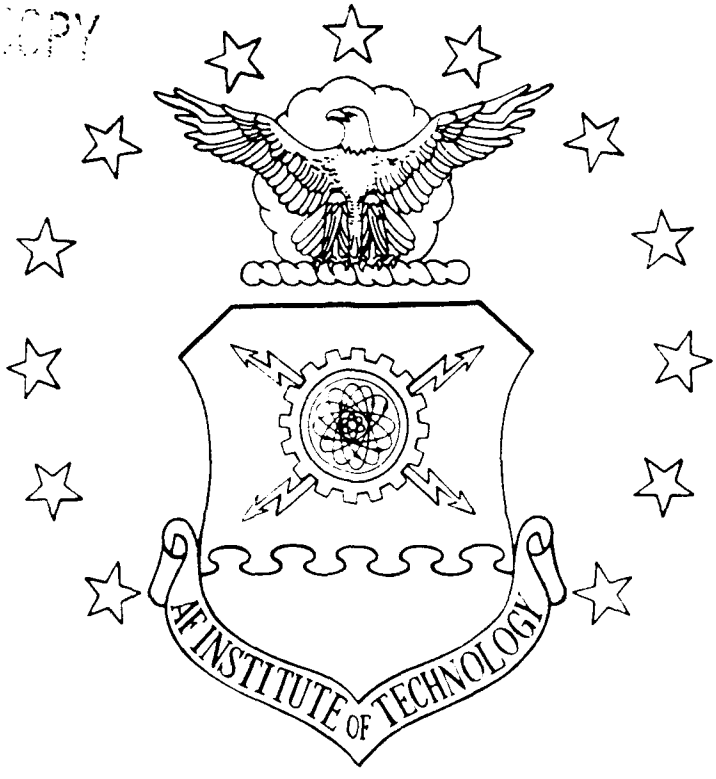

OPERATING CHARACTERISTICS OF XENON GAS DISCHARGES

THESIS

Michael E. Ruark, Captain, USAF

AFIT/GEP/ENP/90D-06

DEPARTMENT OF THE AIR FORCE
AIR UNIVERSITY
AIR FORCE INSTITUTE OF TECHNOLOGY

Wright-Patterson Air Force Base, Ohio

AFIT/GEP/ENP/90D-06

OPERATING CHARACTERISTICS OF XENON GAS DISCHARGES

THESIS

Michael E. Ruark, Captain, USAF

AFIT/GEP/ENP/90D-06

AFIT/GEP/ENP/90D-06

OPERATING CHARACTERISTICS OF XENON GAS DISCHARGES

THESIS

Presented to the Faculty of the School of Engineering

of the Air Force Institute of Technology

Air University

In Partial Fulfillment of the

Requirements for the Degree of

Master of Science in Engineering Physics

Michael E. Ruark

Captain, USAF

December 1990

Preface

This report represents an effort, sponsored by the Plasma Research Group at the Wright Research and Development Center(WRDC), to measure some of the fundamental characteristics of Xenon discharges. The experiment was designed and built from scratch, so that I spent a significant amount of time in the acquisition and set-up of the experiment. Most of the set-up was performed in the previous quarter though, so there was still plenty of time to get lots of data. Two significant problems occurred during the course of the experiment. One was the discovery of an air leak in the discharge tube which rendered most of the data taken in the first two weeks unreliable, except possibly in the characteristics of Xe-N_2 mixtures! The second was a leak in the roof which soaked everything when it rained. The entire experiment was then moved to another room in the building.

I would like to thank both Dr. Alan Garscadden of the Plasma Research Group at WRDC and Dr. William Bailey of AFIT for their patient support and endurance during the course of this experiment. In addition, I would like to thank all of the people and friends at the Plasma Research Group for their support and help during the last 20 weeks. All of the equipment used was borrowed from them.

Finally, I would especially like to thank my wife, Marcia, and dear sons, Justin and Derek, for all of the nonsense and long hours that they had to put up with during the entire course of my AFIT residence. It's not for nothing, sweetheart, and, yes, we can go fishing now, pal.

Table of Contents

List of Figures

Abstract

The voltage-current and spectral line intensity-current characteristics were measured for four Xenon gas discharges. The four discharge configurations were made up of two tubes, each examined at pressures of 1 and 10 Torr. The first tube was a hot filament tube with a 1 cm radius, and the second a cold cathode type tube of radius .3 cm. The intensity of the 6p - 6s(8409Å), 7p - 6s(4624Å), 7d - 6p(7120Å), and 7p - 6s'(7968Å) transitions, and discharge voltage were measured for each configuration for a range of currents and pressures of .2 - 40 mA, and 1 and 10 Torr, respectively. Intensity dependence upon current was primarily linear in all cases with some important deviations. The hot filament tube at 10 Torr showed a large decrease in intensity between 4 and 6 mA in the 8409Å line. This is thought to be connected with the onset of constriction in the discharge at this point. The coincidence of the upper level of this transition with several molecular ion levels of xenon, could account for quenching of this transition. Voltage-current characteristic results were different for the different configurations. A decreasing characteristic was observed for a hot filament cathode tube at both pressures. The voltage for the hot filament tube decreased from 700 to 100 V at 10 Torr, and from 130V to 60V for the 1 Torr case. The decreasing characteristic of the tube at 1 Torr may be due to the combination of gas heating and stepwise ionization mechanisms. Stepwise excitation is also supported by the somewhat quadratic line intensities as a function of current. It is not clear why the voltage of the hot filament tube

decreases by a factor of seven when the current is increased from 1 to 40mA. At 10 Torr the cold cathode tube voltage decreased from about 320V to 260V for currents below 4mA, and then increased to 320V again for currents from 4 to 40mA. At 1 Torr the cold cathode tube voltage increased from 310V to 480V. The increasing characteristic may coincide with the onset of abnormal glow observed at 2 and 20mA for the 1 and 10 Torr cases, respectively. Spectral line intensity oscillations(~ 1kHz) were observed in all cases, typically approaching 90% modulation. Striations were obse ved in all configurations. No clear functional dependence upon current was noted. Increasing the pressure in the cold cathode tube damped the striations significantly. The intensity variation of the standing striations for the cold cathode tube at 1 Torr was about 30%, while at 10 Torr the variatioon only approached about 10 %. Striations were also observed in the hot filament tube but were not measured.

EXCITATION IN XENON DISCHARGES

I. *Introduction*

Purpose of Study

The purpose of this investigation is to examine some of the basic characteristics of four low-pressure Xenon discharge configurations. Two primary discharge characteristics will be measured; (1) voltage-current characteristics, and (2) intensity-current characteristics. The voltage-current characteristics are meant to provide an indication of the discharge mode, estimations of the electric field in the positive column, and provide an idea of the current dependence of the characteristic electron energy in the positive column. The intensity-current characteristics are intended to provide information on the types of excitation and ionization mechanisms occurring in the discharge positive column. In addition, discharge oscillations will be examined to determine their effects on the measurements and the interpretation of the results.

Scope of Work

Two glass discharge tubes will be examined. The first tube is a typical hot filament tube, and the second a small bore col ˙ cathode tube. The initial intensity measurements will consist of a survey of 17 lines in the hot

filament tube at 1 Torr to determine if any anomalies in the trends exist. The measurement will then be refined to a study of 4 representative lines. The four lines examined are the 7d - 6p(7120Å), 7p - 6s(4624Å), 7p - 6s'(7968Å), and the 6p - 6s(8409Å) transitions. The current dependence of the intensity of these four lines will be measured for both the first and second tubes at pressures of 1 and 10 Torr and a current range of .2 to 40 mA. Discharge voltage measurements will be made concurrently with the intensity measurements for each configuration. These measurements will be made at pressures of both 1 and 10 Torr. The intensity of oscillations in the positive column will also be measured for each tube. Variations in the axial intensity for the small bore tube are also examined.

In addition, a third tube will be used only to investigate the effects of radiation trapping at 10 Torr. This tube is different from the others in that windows are mounted on the ends to allow axial intensity measurements. These axial intensity measurements, when compared to radial intensity measurements, allow one to determine the if radiation or photon trapping is occurring.

II. *Background*

Introduction

This chapter is meant to provide the background necessary to understand the measurements taken and the reasoning behind them. Sections 1 and 2 provide some information on the importance of Xenon in various laboratories that motivated the study. Section 3 provides some basic information on the operating characteristics and typical structure of a typical low-pressure glow discharge. Some of the ionization and excitation mechanisms that may be occurring in the positive column of a glow discharge are discussed in section 4, while section 5 takes a brief look at some specific Xenon characteristics. Section 6 provides the basis for the intensity measurements, including a discussion of radiation trapping, and section 7 examines discharge oscillations and their relevance.

Uses and Importance of Xenon

Xenon has a wide variety of applications in high intensity lamps, infrared lasers, and possible uses in radiation detection. There has been a recent resurgence in interest in Xenon lasers due to breakthroughs in scalability made by the Soviets as reviewed by Glessner[1]. Xenon flashlamps are used extensively on Nd:Yag lasers to provide the high intensity light needed to achieve a population inversion. In addition, Xenon has been used in general purpose lamps where very intense light is needed, such as projection lamps and floodlamps. The primary drawback and restriction in

the wide use of Xenon for these purposes is the cost. At the time of this writing the cost for 100 L of 99.995% purity Xenon is about $1700.

DC Discharges

Structure of a Normal Glow Discharge . When a discharge is in the normal glow mode at a given pressure and current, it exhibits a clear structure of visible light and dark regions, hence the name A typical discharge structure for a glow discharge with plane parallel electrodes, although not to scale, is shown in Figure 1. The Aston dark space is typically very thin and is sometimes not discernible to the naked eye, especially above about 1 Torr. In addition, hollow cathode electrodes, or a hot filament cathode may significantly alter the appearance of the various regions. A brief synopsis of each region[2,3] and its important characteristics follows:

Aston's Dark Space . Electrons produced by secondary emission at the cathode, usually of low energy (~ 1eV), are accelerated by a strong electric field. However, the electrons do not yet possess enough energy to excite or ionize

the gas.

Cathode Glow . Weakly luminescent region where electrons have gained enough energy to excite gas molecules. The energy gained corresponds to the maximum of the excitation function.

Cathode Dark Space . (Also referred to as Crooke's dark space)

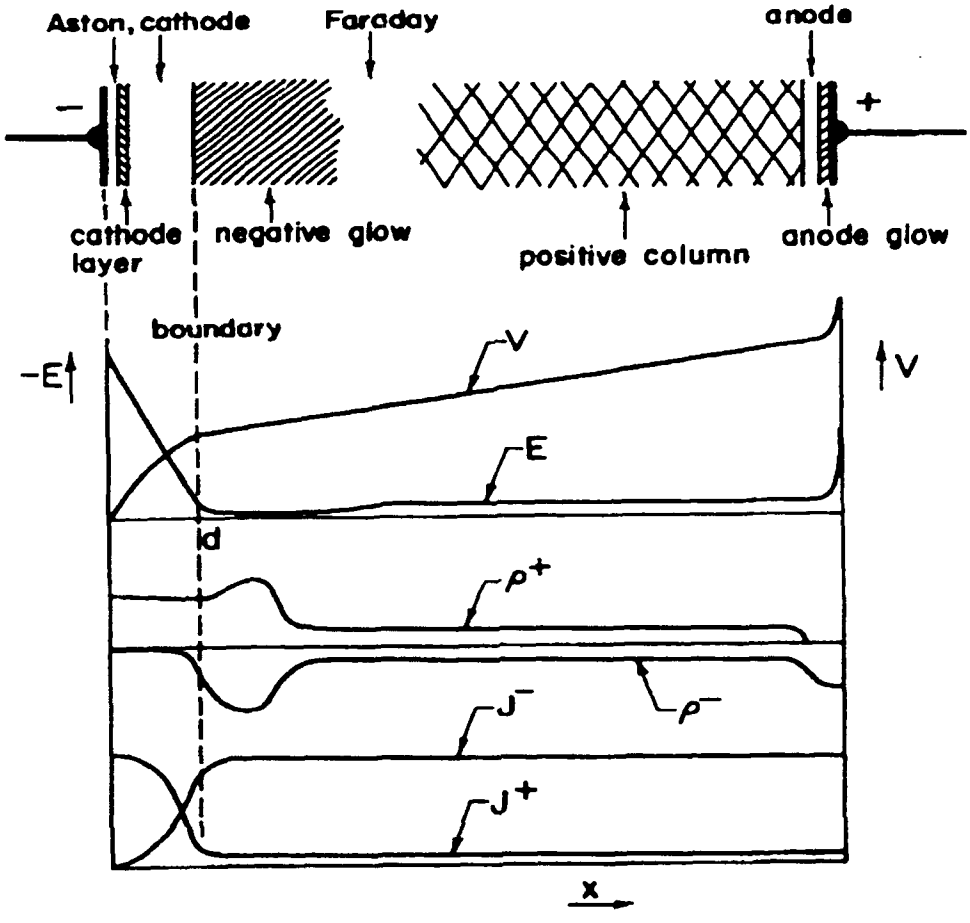

Figure 1 : Glow Discharge Structure, E, V and n_e. Ref: A. von Engel, p.218

This region is characterized by a few slow electrons created by inelastic collisions and many fast electrons whose energy is well past the maximum of the excitation function. Excitation by the slow electrons is responsible for the faint light that may be present in this region, while the fast ones induce highly efficient ionization. This ionization is responsible for strong electron multiplication. This strong electron multiplication and high ionization rate, coupled with the different mobilities of ions and electrons induce a

strong space charge which is responsible for the reduction in the electric field seen here.

Negative Glow . This weak electric field region is characterized by a sharp increase in light output. The electron energy decreases with increasing distance from the cathode. Ionization efficiency is low, but excitation efficiency is large and decreases with increasing distance from the cathode. This effect results in a decreasing luminosity.

Faraday Dark Space . Dark region corresponding to the decrease in electron energy in the negative glow to the point where excitation is negligible.

Positive Column . The electrons from the dark space have gained enough random energy to induce excitation. The drift velocity is now much less than the random thermal velocity, and the electron motion is now random rather than beam-like. The axial component of the electric field is nearly constant, which, by Poisson's equation results in charge neutrality, i.e. $n_e \approx n_i$. The characteristics of the positive column are found to be independent of length.

Anode Dark Space . Electrons are accelerated at the anode, due to the space charge built up here by electron attraction and ion repulsion, and resume a beam-like nature.

Anode Glow . Electrons have gained enough energy to excite and ionize the gas before impacting the electrode.

Before moving on, some general comments are in order. First, any changes in the inter-electrode distance will be taken up by the positive

column, with no effect on the other regions, or the discharge characteristics, unless the anode enters the Crooke's dark space. At this point, ionization becomes more difficult, and the discharge is said to be obstructed. Second, in the interest of definitions, the cathode fall region is defined as the high field region between the cathode and the beginning of the negative glow. This will be important in estimating the positive column voltage, necessary in determining the mean electron or excitation temperature, based on the discharge voltage characteristics. For a Xenon discharge with plane parallel Ni electrodes, the cathode fall voltage is about 160V.

Since the previous discussion applies to plane parallel electrode configurations, some additional modifications are in order for the case of a hot filament discharge. In this case, thermionic emission from a heated filament provides the necessary electrons to sustain the discharge rather than secondary electron emission as in the cold cathode case. The current density provided by the cathode is then[4]

$$j = AT^2 e^{-e\varphi/kT}, \qquad (2)$$

where φ is the cathode material's work function in V, kT/e is the gas temperature in eV, and A is a constant somewhere between 60 and 160 $A \cdot cm^{-2}K^{-2}$. For a tungsten filament at 1800 C, this represents a current density of about 230 mA/cm^2. However, this may not be the actual current flowing since the ejected electrons will tend to set up a space charge layer which will inhibit the emission of more electrons, thereby reducing the current. The actual current flowing in the discharge tube will be governed

by the ability of the electric field between the cathode and anode to pull the electrons out of the electron cloud generated by the hot filament. This field must be high enough to overcome the space charge layer.

The electron energy generally required for the electrons to ionize the gas in the hot filament case is approximately twice the ionization potential[5,6] of the gas. Assuming that the cathode fall voltage represents the electron energy required for ionization, then $V_c \approx 2V_i$. However, the voltage required to overcome the space charge layer is governed by the Child-Langmuir law, which states that the current density between two plane electrodes in a high vacuum is proportional to $V^{3/2}/d$, where d is the sheath distance. Therefore the actual cathode fall voltage for the cathode layer in the hot filament discharge will be somewhere between $2V_i$ and the voltage governed by the Child-Langmuir law. For a filament providing 230mA/cm^2, and a cathode fall distance of 1cm, the voltage required to maintain this current density is about 140V.

Electron Gain and Loss Mechanisms in the Positive Column: Schottky Theory

So far, some basic characteristics of a low-pressure gas discharge have been discussed. However, since this study is concerned with the measurement of intensity in the positive column, which represents excited state densities and how they vary with current (i.e. electron density-drift velocity product), it is necessary to examine the basic kinetic mechanisms in a discharge. For example, it is known that ionization occurs in the

column, but what kind of ionization? Are only neutral atoms ionized, or is it possible that excited atoms are being ionized also? Step-wise ionization and excitation can play an important role in the positive column, and may alter some of its basic characteristics. These and similar issues are addressed in this section.

As stated earlier, within the positive column the electrons have lost their beam-like nature and move around in a rather random fashion, drifting towards the anode, where the random thermal velocity is much greater than the drift velocity. In addition, since the electric field in the positive column is approximately constant, then the charge density and the derivative of the electric field are related by Poisson's equation:

$$d^2V/d^2x = -4\pi(n_i - n_e) = 0 , \qquad (3)$$

which leads to

$$n_i \approx n_e \approx n , \qquad (4)$$

or charge neutrality, where n_e and n_i are the electron and ion densities, respectively.

Electron Gain Mechanisms . Electron impact ionization is assumed to be the primary electron production mechanism within the column,

$$N_g + e^- \text{---> } N_g^+ + e^- + e^- , \qquad (5)$$

or,

$$N_g^* + e^- \text{---> } N_g^+ + e^- + e^- , \qquad (6)$$

where N_g is the neutral gas atom, N_g^* is a excited electron, and e^- is the electron. The first equation represents single-step ionization from the ground state, while the second equation represents ionization from an

already excited state. More important to the discussion is the ionization frequency, which is generally given as,

$$Z = n_e N_g R_{gi} = n_e N_g < Q(v)v > , \qquad (7)$$

where Q(v) is the ionization cross-section, which is generally a function of electron energy, and < > represents the integration over the appropriate electron energy distribution. The form of the ionization rate coefficient, R_{gi}, can become quite complicated depending on the form of the distribution and the form of the cross section. In the following discussion it is assumed that the distribution is Maxwellian. Furthermore, it should be noted that the following discussion applies to cases where; P ~1 -10 Torr, R~1 -10 cm, and I~.10^{-4} - 1 Amps. Beyond these limits the Schottky theory breaks down.

Electron Loss Mechanisms . Three types of electron loss mechanisms can occur in the column: diffusion, recombination, and/or attachment[7]. All three will likely be occurring in the discharge at any given time, but which one is dominant will depend primarily upon the gas and the pressure in the tube. Recombination, the creation of a neutral from a collision between an electron and an ion, is governed by the relative charge densities and the recombination coefficients of the discharge constituents, and may or may not be important. Attachment, the creation of a negative ion from a collision between an electron and a neutral gas molecule, is restricted to electronegative gases, which Xenon is not, and shall be neglected. For the purposes of the following discussion, diffusion is assumed to be the dominant electron loss mechanism within the positive column.

Diffusion is the mechanism by which particles in a high concentration

area move to an area of lower concentration. The diffusion velocity in one direction is given by

$$v = - (D/N)dN/dx , \qquad (8)$$

where D is the free diffusion coefficient for the particle of interest (cm^2/s), N is the gas density(cm^{-3}), and dN/dx is the density gradient. The situation is somewhat more complicated when both ions and electrons are present in equal numbers, as in the positive column. This complication arises primarily from the coulomb interaction between the electrons and ions.

When both electrons and ions are present in a common electric field, the electrons tend to diffuse faster then the heavier ions. This space charge separation sets up a radial electric field which in turn tends to slow the electrons down. The net result is that the ions and electrons can be thought of as drifting at some net speed, called the ambipolar drift velocity,

$$v_a = v^+ = v^- , \qquad (9)$$

where v+,- is the ion and electron drift velocity respectively. Applying eq. (8) to both the ions and electrons yields

$$v_a = - \frac{D_a \, dN}{N \, dx} , \qquad (10)$$

where

$$D_a = \left[\frac{D^+\mu^- + D^-\mu^+}{\mu^+ + \mu^-} \right] , \qquad (11)$$

where $D^{+,-}$ and $\mu^{+,-}$ are the ion and electron diffusion coefficients and mobilities, respectively. If, as in the case of the positive column, the mobility and the temperature of the electrons is much greater then that of

the ions, then

$$D_a \approx T_e \mu^+ , \tag{12}$$

where T_e is the electron temperature in eV.

Gain and Loss Balance . Now that the dominant electron loss and gain mechanisms have been examined, some of the important discharge characteristics, such as T_e, and E_z, can be determined. Applying charge neutrality and assuming a cylindrical geometry[8] the number of particles leaving a volume element dr is given by,

$$dZ_{diff} = 2\pi r D_a \left[\frac{1}{r} \frac{dN}{dr} + \frac{d^2N}{dr^2} \right] dr . \tag{13}$$

This diffusion loss must be balanced by ionization for the element dr. Defining the ionization frequency as,

$$dZ_i = 2\pi r Z' n dr , \tag{14}$$

where the form of Z' depends upon the ionization mechanisms involved, and equating equations (13) and (14), the result is a second-order Bessel equation

$$\frac{d^2n}{dr^2} + \frac{1}{r}\frac{dn}{dr} + \frac{Z'n}{D_a} = 0 \tag{15}$$

Solution of this equation applying boundary conditions, $N(0) = N_0$, and $N(R) = 0$, yields the result for the first eigenvalue of the Bessel function

$$Z'/D_a = (2.405/R)^2 . \tag{16}$$

The information determined by Eq (16) is determined by the form of the ionization frequency, Z'. The two cases that will be considered here are single-step ionization, and step-wise ionization.

Single-step Ionization . In single step ionization, as the name implies, electrons are produced solely by ionization from the ground state, and are not formed by the ionization of an excited state. The rate of ionization can be a somewhat complicated function of electron temperature, depending upon the electron energy distribution. The general idea can be conveyed, however, if one assumes a Maxwellian electron energy distribution. The rate coefficient, R_{gi}, is then the integration of the ionization cross section over the distribution function

$$Z = n_e N_g R_{gi} = n_e N_g < Q(v)v > , \qquad (7)$$

The ionization cross section can be approximated by the linear ramp

$$Q(\varepsilon) = \beta(\varepsilon - \varepsilon_i) , \qquad (17)$$

where β is the slope of the cross-section, ε is the electron energy in eV, and ε_i is the threshold ionization energy in V. Integrating this cross-section over a Maxwellian energy distribution yields, for R_{gi}

$$R_{gi} = \alpha\beta(T_e)^{1/2}(\varepsilon_i + 2T_e)e^{-\varepsilon_i/T_e} , \qquad (18)$$

where

$$\alpha = \left(\frac{8 \cdot 1.6 \cdot 10^{-12}}{\pi m}\right)^{1/2} , \qquad (19)$$

and T_e is in eV. Balancing the ionization rate with the electron diffusion losses, as in Eq (16), and substituting the appropriate relations for D_a and Z, results in the electron temperature being dependent only upon the pressure radius product. This shows that the electron temperature in the positive column is a unique function of the pressure-radius(PR) product and the characteristics of the particular gas. For example, the electron

temperature, T_e, as a function of PR for a xenon discharge (ε_i = 12.1 V, $\beta = 10^{-15}/(2\varepsilon_i)$ cm^2/V) ,as shown in Figure 2. The important point to be made here in relation to this experiment is that, under the assumptions made, Te is independent of current. Therefore, as long as single step ionization and ambipolar diffusion were the dominant electron gain and loss mechanisms in the discharge, changing the discharge current would not change the electron temperature.

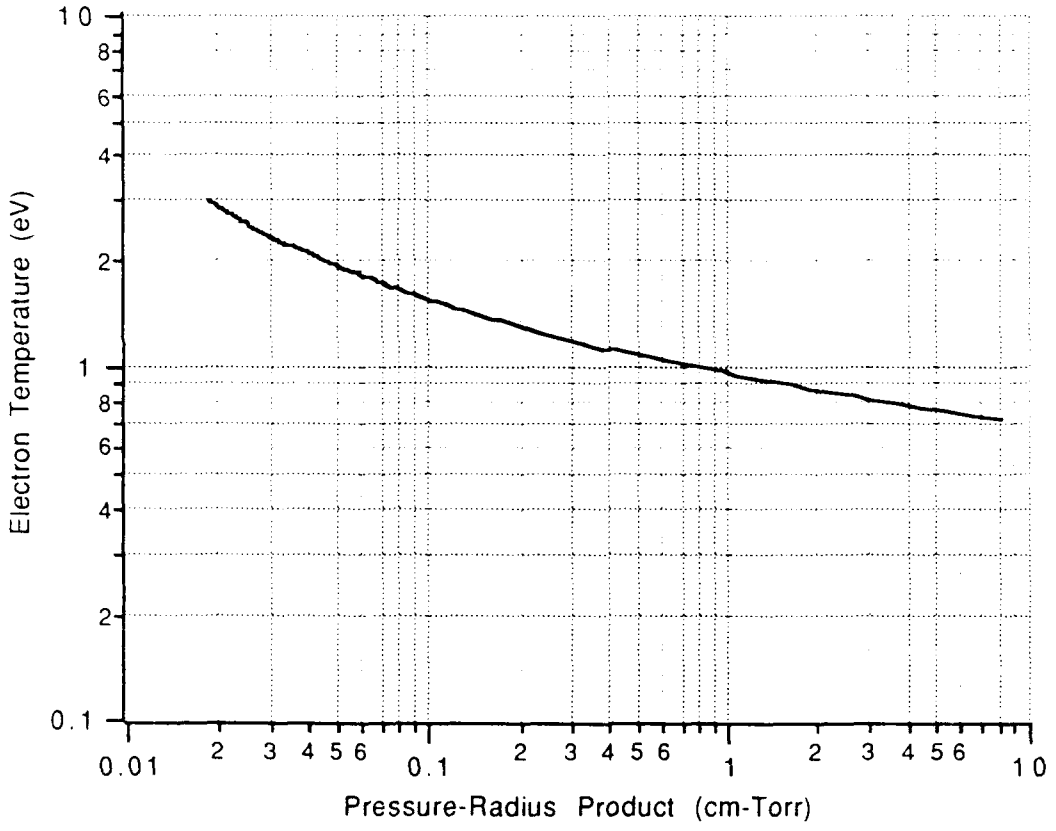

Figure 2: Te vs PR for Xenon

In addition, the relationship between Te and E/N can be determined by balancing the energy the electrons gain from the field and the energy they

lose in collisions. For elastic collisions[9]

$$E/N = 3Te(2\kappa)^{1/2}/\lambda_1 \quad (10^{-17} V\ cm^2) \qquad (20)$$

where $\kappa = (2m/M)$ and λ_1 is the electron mean free path at 1 Torr. This means that for a given gas pressure, the electric field in the positive column is also independent of current.

Since the discharge voltage is the sum of the cathode fall voltage and the positive column voltage, then measuring the discharge voltage can provide information of the electric field in the positive column if the cathode fall voltage is known. As stated before, the cathode fall voltage is constant in a normal glow discharge. Therefore, the voltage across the positive column can be determined by subtracting the cathode fall voltage from the discharge voltage. In a normal glow discharge, under these conditions, the discharge voltage should remain constant throughout the current range.

If inelastic collisions are occurring, but single step mechanisms are still dominant, then the E/N may increase since more energy is required to balance that lost in inelastic collisions. For example, considering Xenon at PR =1 (P=1 Torr), from Figure 2, Te≈ 1 eV. The mean free path, λ_1, is then about 5.6×10^{-3} cm, and $\kappa = 2m/M = 8.4 \times 10^{-6}$. This results in an electric field of about .5V/cm. For a positive column about 60cm long, this corresponds to a voltage of about 30V. On the other hand, if inelastic losses are present, then the fraction of energy lost may be somewhat higher. If κ is on the order of 10^{-3}, then this may represent about an order of magnitude increase in the electric field, and a corresponding voltage of about 300V.

Consider the effects of pressure changes in the discharge on the positive column voltage. If the pressure in the tube is arbitrarily increased from 1 to 10 Torr in a tube of radius 1 cm, what will be the corresponding effect on the column voltage? From Figure 2, one can see that increasing the pressure from 1 to 10 Torr increases PR from 1 to 10 cm-Torr. This changes the electron temperature from about .9 to about .7 eV. Since this does not represent a very large change, and since E/N is directly related to T_e, then E/N must not change very much either. If N increases by a factor of ten, then the electric field must also increase by a factor of ten.

Step-wise Ionization . The previous section explained the mechanisms involved in a positive column for single-step ionization. In real systems, this may not be the case. The existence of metastable states, states with very long radiative lifetimes, provide an easy step for ionization. There may be a high probability then, that the excited atom may be ionized before it is collisionally quenched by other neutrals or diffuses out of the volume element. This additional ionization term in the balance equation may significantly alter the column characteristics, depending on the metastable state density, the ionization rate and the electron density, and what other mechanisms are playing a role in the discharge.

In order to examine this effect, consider the four-level system shown in Figure 3. The letters g, m, e, and i, correspond to the ground, metastable, excited, and ionic states, respectively. Figure 3 represents a simplified version of Xenon energy level diagram. Let R_{xy} represent the rate

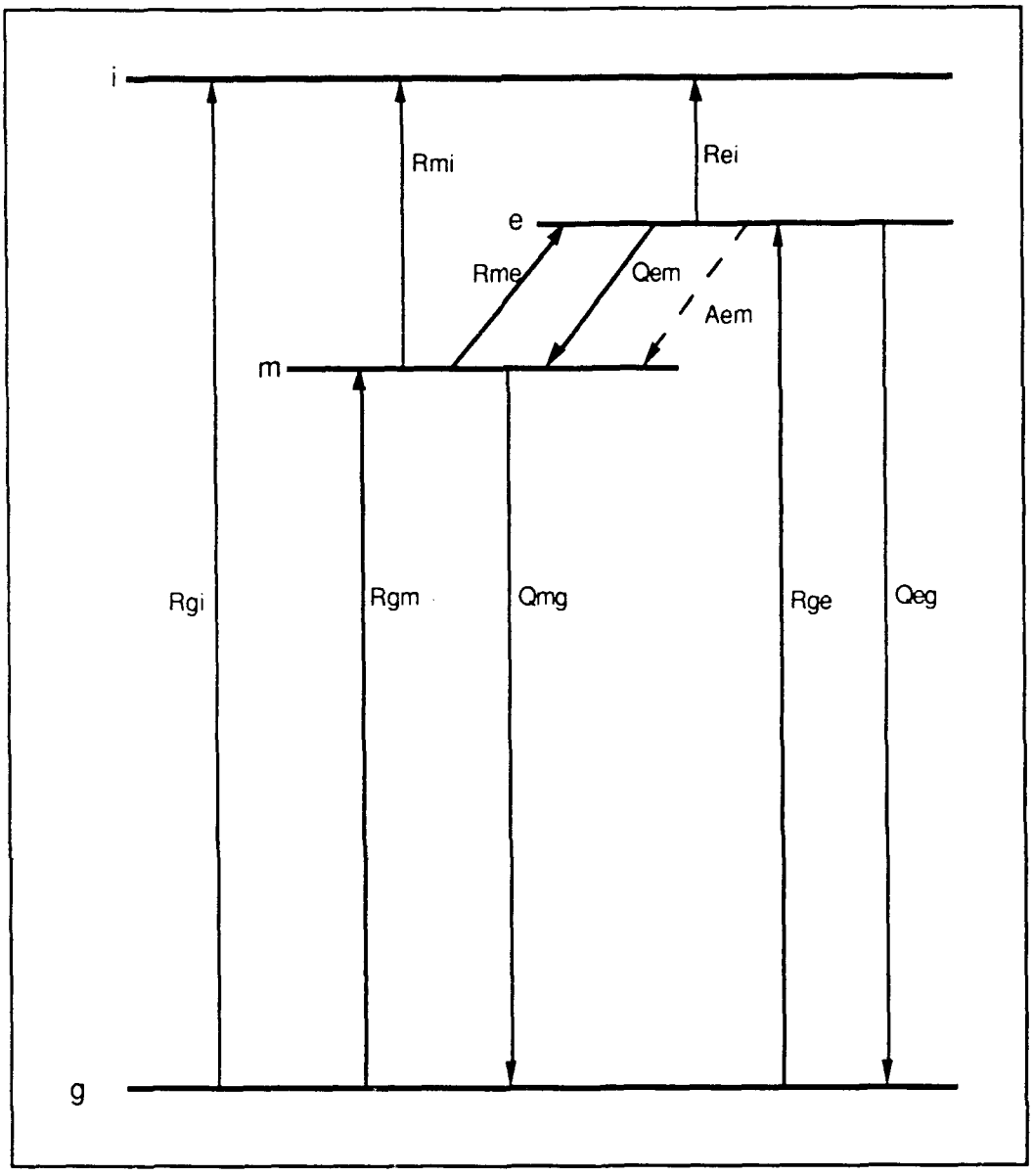

Figure 3: Simplified four-level energy level diagram.

coefficient (cm^3/s) for electron impact transfer between states x and y. It is initially assumed that volume recombination is negligible, and that the radiatively allowed excited state does not suffer significant diffusion losses. Since it is assumed that ionization is occurring from both the excited and

metastable states, the diffusion balance equation now looks like

$$D_a(2.405/R)^2 = N_g R_{oi} + N_m R_{mi} + N_e R_{ei}. \qquad (21)$$

This relation is not so simple to evaluate since the total ionization frequency is now dependent upon both the excited and metastable state,which are in turn dependent upon the electron density. However, a general idea of the trends that may be expected can be at least discussed by considering the state densities involved.

The steady state rate equations for the excited and metastable states are

$$dN_e/dt = n_e N_g R_{ge} + n_e N_m R_{me} \qquad (22)$$
$$- N_e[\, n_e(R_{eg} + R_{em} + R_{ei}) + N_g(Q_{eg} + R_{em}) + A_{em}]$$
$$= 0,$$

and,

$$dN_m/dt = n_e N_g R_{gm} + N_e A_{em} + N_g N_e Q_{em} + n_e N_e R_{em} \qquad (23)$$
$$- N_m[\, N_g Q_{mg} + n_e(R_{me} + R_{mi} + R_{eg}) + D_m'] = 0,$$

where the terms are as follows:

$n_e N_g R_{ge}$ and $n_e N_g R_{gm}$: Electron impact excitation frequency per unit volume from the ground state to the excited and metastable states, respectively.

$_e N_m R_{me}$: Electron impact excitation from the metastable state to the excited state.

$n_e N_e R_{ei}$ and $n_e N_m R_{mi}$: Electron impact ionization from the excited and metastable states.

$N_eN_gQ_{eg}$ and $N_mN_gQ_{mg}$: Binary quenching of the excited and metastable states.

$N_eN_gQ_{em}$: Binary quenching of the excited to the metastable state.

$n_eN_eR_{eg}$ and $n_eN_mR_{mg}$: Superelastic de-excitation of the excited and metastable states.

$n_eN_mR_{em}$: Superelastic de-excitation of the excited to the metastable state.

N_eA_{em} : Spontaneous emission of the excited state.

N_mD_m' : Metastable diffusion.

Note that D_m' is given by $D_m(2.4/R)^2$, where R is the tube radius. Rearranging these equations to solve for the excited and metastable densities yields the result of

$$N_m = \frac{n_eN_gR_{gm} + N_eA_{em} + N_gN_eQ_{em} + n_eN_eR_{em}}{N_gQ_{mg} + n_e(R_{me} + R_{mi}) + D_m'} , \qquad (24)$$

and,

$$N_e = \frac{n_eN_gR_{ge} + n_eN_mR_{me}}{n_e(R_{ei} + R_{em}) + N_g(Q_{eg} + Q_{em}) + A_{em}} , \qquad (25)$$

It is clear from these two equations and the diffusion balance equation that a number of different possibilities could exist depending on what the dominant production and loss mechanisms were for a particular state. Generally, some of these terms can be neglected based on a comparison of the threshold energies and densities of the various states being considered. A detailed analysis of all the possibilities is beyond the scope of this study and could possibly be the sole subject of a fairly thick book. However, some

comments are in order. First, as explained before, the ambipolar diffusion coefficient is linearly related to T_e, while the excitation and ionization rate coefficients are exponentially related. This means that the rate coefficients are much more sensitive to changes in T_e than the diffusion rate. Therefore, with the onset of step-wise ionization a corresponding decrease in the electron temperature would have to occur to maintain the balance. Since E/N is still related to Te, although not strictly linear[10], it is then expected that the electric field, assuming a constant pressure will also decrease with the onset of stepwise mechanisms. In addition, Te may no longer be solely dependent upon the PR product alone. It is possible that under some conditions, the electron temperature may be current dependent. One such condition may be where both the metastable and excited states are collisionally populated, but quenched by neutrals, a likely situation since the neutral population is large ($\sim 10^{16}$ -10^{17} cm^{-3}).

So far, some of the basic characteristics of discharges have been discussed. This provides some of the basic information useful in understanding just what sort of behavior the discharge is supposed to exhibit. It is now necessary to take a brief excursion into specific Xenon characteristics to avoid confusion in notation used later and also to provide further insight as to what behavior Xenon discharges exhibit.

Xenon Characteristics

Xenon Properties . The following is a list of some of the basic properties of Xenon.

Atomic Number:	54
Atomic Weight:	131.30 amu
Density (Gaseous):	5.8971 g/l @STP
Freezing Point:	165.04°K
Specific Heat :	.038cal/g/°K @20°C and constant pressure
Thermal Conductivity:	.000012 cal/cm^2/cm/s/°K @20°C
Ionization Potential:	12.2 eV
Heat Capacity:	4.97 cal/°K/mole @25°C and const. pres.

Energy Levels . A Xenon energy level diagram is shown in Figure 4. The 6s'$[1/2]_0$ and 6s$[3/2]_2$ states, the two lower states of each 6s manifold, are metastable states, while the 6s'$[1/2]_1$ and 6s$[3/2]_1$ states are resonant states. In Figure 4, the resonant states are the upper levels of the 6s and 6s' states while the metastables are the lower levels. Transitions between the metastable and ground states are optically forbidden, that is, an atom in the metastable state cannot spontaneously decay to the ground state. Resonant states are those states in which a transition to the ground state is immediately followed by an optical transition back to the same state[11]. This is different from fluorescence which involves a transition from one state to another, followed by a transition to a different state.

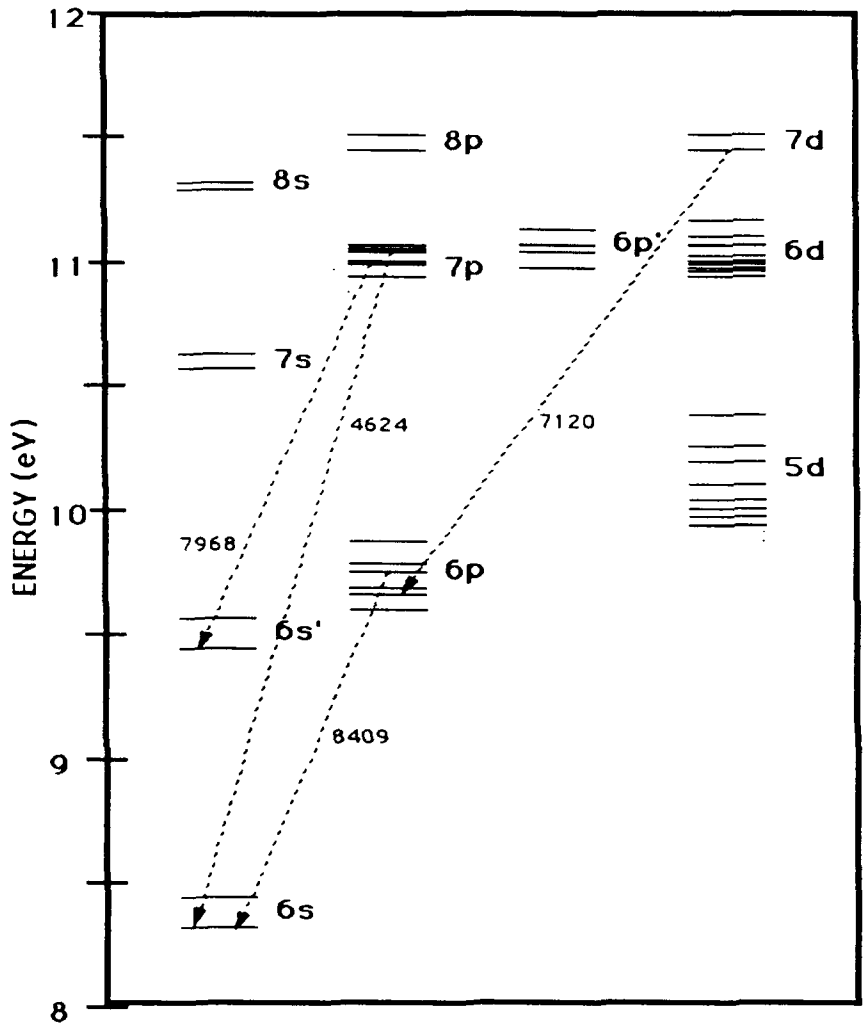

Figure 4: Simplified Xenon energy level diagram. Dashed lines are representative transitions and their wavelengths (Å)

Note the energy level spacing in Figure 4. The resonant and metastable states are at about 8.5 to 9.5 eV, while the ionization level is at 12.1 eV. This

is characteristic of most rare gases. The excited states are usually very close to the ionization threshold. This situation has serious implications in the ionization mechanisms and in the coupling.

Coupling . The noble gases are subject to a peculiar type of angular momenta coupling scheme referred to a *jl* or pair coupling, generally occurs when the excited states are a large distance away from the atomic core. This results in the spin-orbit interaction between the core electrons being much greater than the electrostatic interaction between the core electrons and the excited electrons. This results in a novel spectroscopic notation for the noble gases. Let the atomic core be characterized by angular quantum numbers $\mathbf{L}_c$, $\mathbf{S}_c$, and $\mathbf{J}_c$, where **L**,**S**,and **J** represent the angular momentum, the spin, and the total angular momentum, respectively, and the subscript c represents the atomic core. Let **l**,**s**, and **j** denote the momenta of the outer electron. In general , the total angular momentum of the core couples with the angular momentum of the outer electron to yield a new quantum number **K**, where $\mathbf{K} = \mathbf{J}c + \mathbf{l}$. This **K** couples to the spin of the outer electron to yield the total angular momentum of the system, $\mathbf{J} = \mathbf{K} + \mathbf{s}$. The notation for these states is given by either $nl[\mathbf{K}]_J$ or $nl'[\mathbf{K}]_J$, where n is the principle quantum number. The presence or absence of the prime indicates that $\mathbf{J}c = 1/2$ or 3/2, respectively.

Selection Rules for Noble Gas Transitions . In general, the selection rules for noble gas optically allowed transitions are similar to those in LS coupling schemes. The predominant rule is that $\Delta J = \pm 1$, or 0 if $J \neq 0$ [12]. This rule is never violated. The other rule is that $\Delta L = \pm 1$. Some very faint

transitions can be observed which, in fact, violate this rule, but it is generally obeyed.

Spectral Line Intensity

Excited State Dependence upon Electron Density . It is a well known fact that the intensity (power radiated per unit solid angle) of a spectral line for a transition between upper state *k* and lower state *i* is given by[13]

$$I = \frac{1}{4\pi} N_k \cdot V \cdot h\omega_{ki} \cdot A_{ki} \ , \qquad (26)$$

where N_k is the upper state density, A_{ki} is the transition probability, ω_{ki} is the transition frequency, and V is the volume of the emitting source. This relation assumes that the upper state density is uniform throughout the volume, and that the source is optically thin, i. e. the emitted radiation is not reabsorbed on its way out of the medium. It is clear from this relation for a given volume and transition, the intensity is proportional to the upper state density. As shown before, the excited state density is related to many factors;

$$N_e = \frac{n_e N_g R_{ge} + n_e N_m R_{me}}{n_e(R_{ei} + R_{em}) + N_g(Q_{eg} + Q_{em}) + A_{em}} \ . \qquad (25)$$

For single step excitation and radiative decay the intensity would be linearly proportional to the electron density only. On the other hand, if stepwise mechanisms are dominant, then the intensity is also proportional to the metastable density, where

$$N_m = \frac{n_e N_g R_{gm} + N_e A_{em} + N_g N_e Q_{em} + n_e N_e R_{em}}{N_g Q_{mg} + n_e(R_{me} + R_{mi}) + D_m'} \quad , \qquad (24)$$

as defined before. It is clear then that the intensity may also be quadratically dependent upon the current under the right conditions. Such a condition might be where ground state excitation and quenching are the dominant production and loss mechanisms for the metastable state, respectively. In general, if the diffusion balance equation is electron density dependent, that is, if T_e is current dependent, neglecting W_d, then the intensity should be quadratically dependent upon the current.

The current, on the other hand, is defined as

$$I = en_e W_d(T_e)A, \qquad (27)$$

where e is the electronic charge,n_e is the electron density, W_d is the electron drift velocity, and A is the cross-sectional area of the column. Hence, the electron density is directly proportional to the current, provided that single-step ionization is occurring and T_e doesn't vary, i. e. the drift velocity is constant. If stepwise mechanisms are prevalent, then a proper accounting of the drift velocity must be made. Patrick[14], et al., has determined the electron drift velocity dependence upon E/N in Townsend drift tube experiments. Over the range of E/N of .1 to 100 Td, the drift velocity shows both a sublinear (i.e. n_e^x, where $x < 1$) and linear dependence, and varies by about one order of magnitude over this range.

Equations (25) and (27) form the basis for the measurement of spectral line intensities as a function of current. Measuring the current dependence of the intensity yields the electron density dependence of the excited

state density. It should be made clear, however, that these relations are derived under ideal conditions. There are two factors (at least) which may seriously affect the measurements and their subsequent interpretation. The first is radiation or photon trapping, whereby a photon is reabsorbed before leaving the vessel, thereby decreasing the observed intensity. Secondly, discharge oscillations may affect the results. The presence of striations, stationary regions of varying intensity, is well recorded in rare gas discharges[15]. To make matters worse, moving striations (~ 1-3kHz), not discernible to the naked eye, may also be present. These details are the subjects of the next two sections.

Radiation Trapping . Radiation or photon trapping is the mechanism by which photons emitted from a gaseous medium are quickly reabsorbed in the medium before escaping the container. Since the intensity measured is proportional to the number of photons emitted, then radiation trapping could significantly affect the intensity measurements and subsequent interpretation of the data. Transitions which terminate upon a metastable or ground state are particularly vulnerable. Trapping increases the effective lifetime of a particular transition, by increasing the relative amount of time that an atom stays in the upper state due to repeated reabsorption. This in turn could significantly decrease the measured intensity. Any measurement which relies on the ratio of intensities of two transitions, or the absolute intensity of a transition, could be seriously affected by radiation trapping. The following discussion provides an idea of the possible significance of this error.

Corney[3] has examined the change in intensity of an approximately collimated beam of radiation confined to solid angle $d\Omega$ as it propagates through a gas of excited atoms. The assumptions made are that the state densities and the lineshape factor are constant within the medium. Reviewing briefly, the radiative transfer equation is given as

$$\frac{dI_\omega}{dt} = \frac{h\omega}{4\pi}\left[A_{ki}N_k + \left(B^I_{ki}N_k - B^I_{ik}N_i\right)I_\omega\right]g(\omega) = \varepsilon_\omega - k_\omega I_\omega \,, \qquad (28)$$

where

$$k_\omega = \frac{h\omega}{4\pi}B^I_{ik}N_i\left(1 - \frac{g_i N_k}{g_k N_i}\right)g(\omega) \approx \frac{\lambda^2 g_k}{4\, g_i}A_{ki}N_i g(\omega) \,, \qquad (29)$$

and

$$\varepsilon_\omega = \frac{h\omega}{4\pi}A_{ki}N_k\, g(\omega) \,, \qquad (30)$$

where the relations,

$$B^I_{ik} = \frac{4\pi}{c}B^\rho_{ik} \,, \quad B^\rho_{ik} = \frac{\pi^2 c^3 g_k}{h\omega^3_{ki}\, g_i}A_{ki} \,, \quad \text{and} \quad \omega = \frac{2\pi c}{\lambda} \,, \quad g_i B^I_{ik} = g_k B^I_{ki} \,, \qquad (31)$$

have been used. The superscripts ρ and I represent the coefficients with respect to radiation density and intensity respectively. A_{ki}, B_{ki}, and B_{ik}, are the spontaneous and stimulated emission and absorption coefficients, respectively, $g(\omega)$ is the lineshape factor, where ω is the frequency. It is assumed that no population inversion exists ($g_i N_k << g_k N_i$).

Using the assumptions stated and considering the gas as a slab bounded by x=0 and x=L, the solution to Eq (28) is

$$I_\omega(L) = I_\omega(0)e^{(-k_\omega L)} + \frac{\varepsilon_\omega}{k_\omega}\left(1 - e^{(-k_\omega L)}\right) \,, \qquad (32)$$

where $\varepsilon_\omega/k_\omega$ is called the source term, and $k_\omega L$ is referred to as the optical

thickness. By setting the incident intensity, $I_\omega(0)$, equal to zero, then $I_\omega(L)$ represents the emission and self-absorption in a volume element of a gas discharge,

$$I_\omega(L) = \frac{\varepsilon_\omega}{k_\omega}\left(1 - e^{(-k_\omega L)}\right) . \qquad (33)$$

The lineshape factor at the transition frequency, assuming a Doppler line profile, is given as

$$g(\omega) = \frac{2}{\Delta\sqrt{\pi}} \exp\left[-4(\omega-\omega_{ki})^2/\Delta^2\right] , \text{ where } \Delta = \frac{2\omega_0}{c}\sqrt{\frac{2kT}{M}} , \qquad (34)$$

where M is the atomic mass and T is the gas temperature. Finally, substituting in Eq (27), (28), (31), and (34) into Eq (33) yields the desired relation

$$I_\omega(L) = \frac{h\omega^3 \ (1 - \exp(-k_\omega L)}{4\pi^3 c^2 (N_i g_k / N_k g_i - 1)} . \qquad (35)$$

Some statements concerning Eq (35) and radiation trapping can now be made. If the optical thickness is much less than one, the exponential term can be expanded and

$$I_\omega(L) \approx \varepsilon_\omega L = \frac{h\omega}{4\pi} A_{ki} N_k \, g(\omega) L , \qquad (36)$$

and the intensity is linearly related to the excited state density, and L, for a given transition. However, as the optical thickness approaches unity, self absorption becomes strong and the intensity increases more slowly. As an example, consider the case where the line intensity ratio method is used to determine the electron temperature. Assuming the medium is optically thin, the intensity ratios can be written as to be dependent only upon electron temperature

$$\frac{I_1}{I_2} = \frac{\lambda_2 A_1 R_{g1}}{\lambda_1 A_2 R_{g2}}, \qquad (37)$$

where single-step excitation, and emission from the same upper state have been assumed. Since the rate coefficients are explicit functions of mean electron temperature, and if the A coefficients are known, then the intensity ratio can be used to determine the mean electron temperature in the gas. However, if the optical thickness approaches unity, then the intensity ratio is also a function of length. In addition, since k_ω is dependent upon the lower state density, metastables, with their relatively higher concentrations , would be more susceptible to trapping than transitions which terminated on a radiatively allowed state.

As an example, Figures 5 and 6 show the variation of the ratio of intensities for the 4624Å , 7120Å , and 8409Å lines for electron densities of 10^{10} and 10^{12} cm^{-3}, respectively. Line #1 represent the ratio 8409Å/7120Å, line #2 represents the ratio 4624Å/7120Å, and line #3 represents the ratio 8409Å/4624Å. The excited and metastable densities were assumed to be linearly related to the electron density, based on available rate coefficients. At the lower electron density, the material is optically thin and the ratio of intensities is independent of the tube length. However, at the higher electron density of 10^{12} cm^{-3}, the intensity ratio becomes significant for different tube lengths, decreasing by almost 50% between 1 and 30 cm. Note that the ratio between the 7120Å line and the other two lines show significant change while the ratio between the 4624Å and 8409Å lines show little length dependence. This is primarily because the optical thickness for

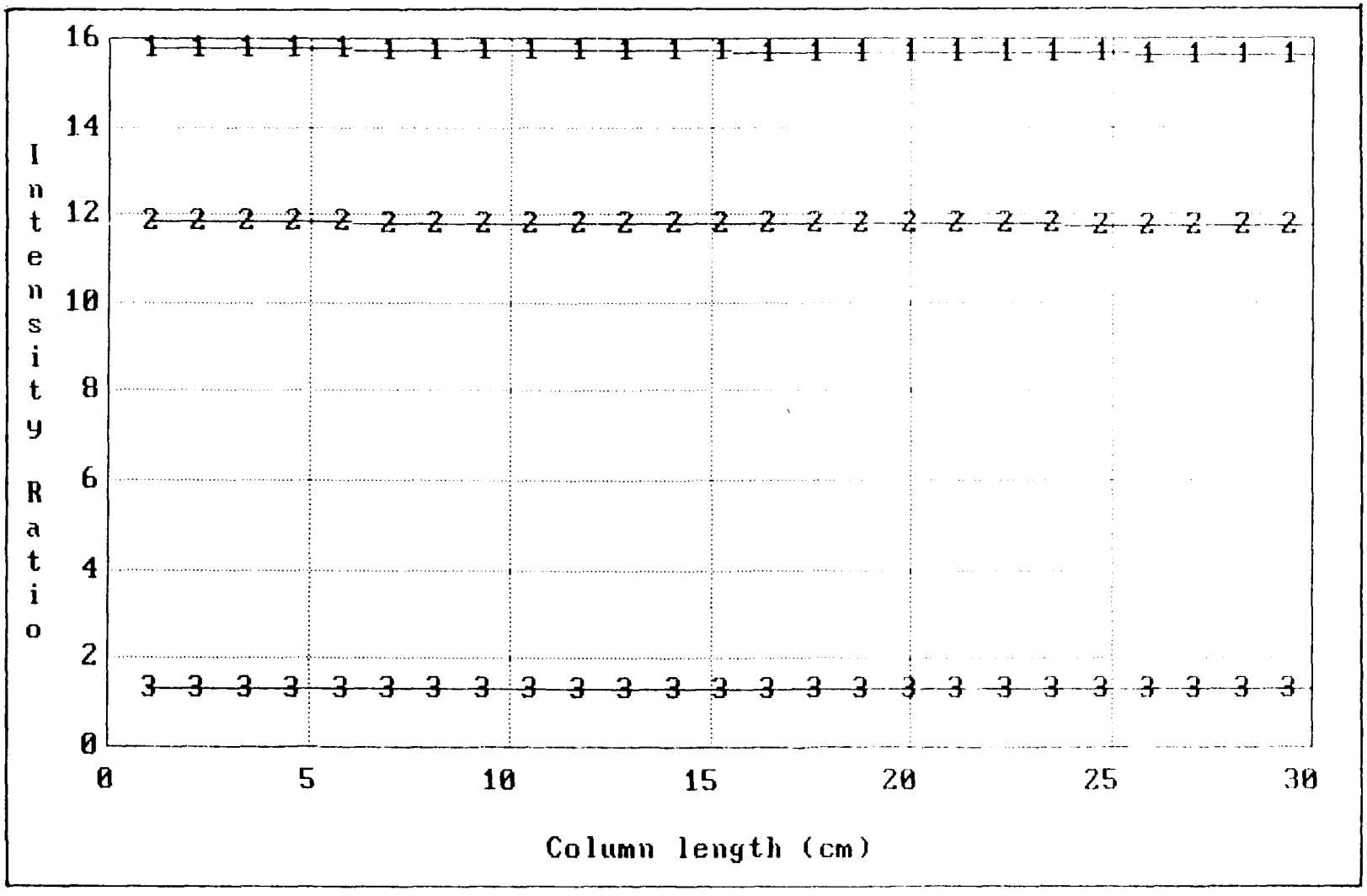

Figure 5: Ratio of Intensities of Spectral Lines as a Function of Positive Column Length. ne = 1E10. Line #1 is 8409/7120A, Line #2 is 4624A/7120A, and Line #3 is 8409A/4624A.

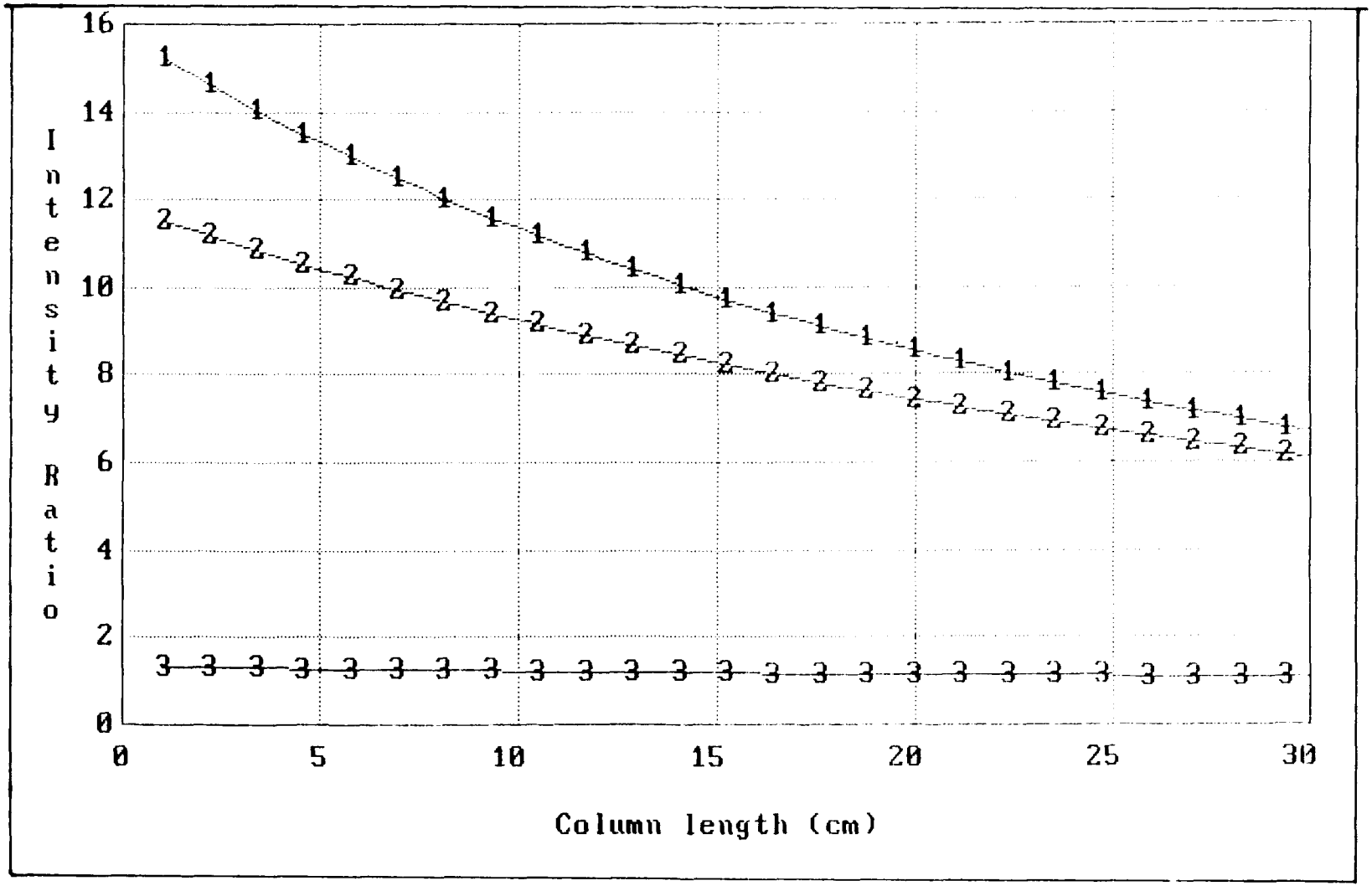

Figure 6: Ratio of Intensities of Spectral Lines as a Function of Positive Column Length. n = 1E12. Same notation as Figure 5.

the 7120 line is not length dependent at this density, as shown in figure 7, since the 7120A transition terminates on an excited state and not on themetastable state. The larger metastable density increases the optical thickness of the 4624A and 8409A transitions by at least an order of magnitude. Figure 8 shows the dependence of the ratios upon the electron density for a fixed length. It is clear from this figure that radiation trapping would tend to be more prevalent at the higher current densities. This is due to the increase state densities at the higher currents.

The previous section has shown how radiation trapping can effect the measurement of intensity and subsequent calculations, such as T_e. In the next section, another type of intensity variation which also has serious implications in intensity measurements is examined: discharge oscillations.

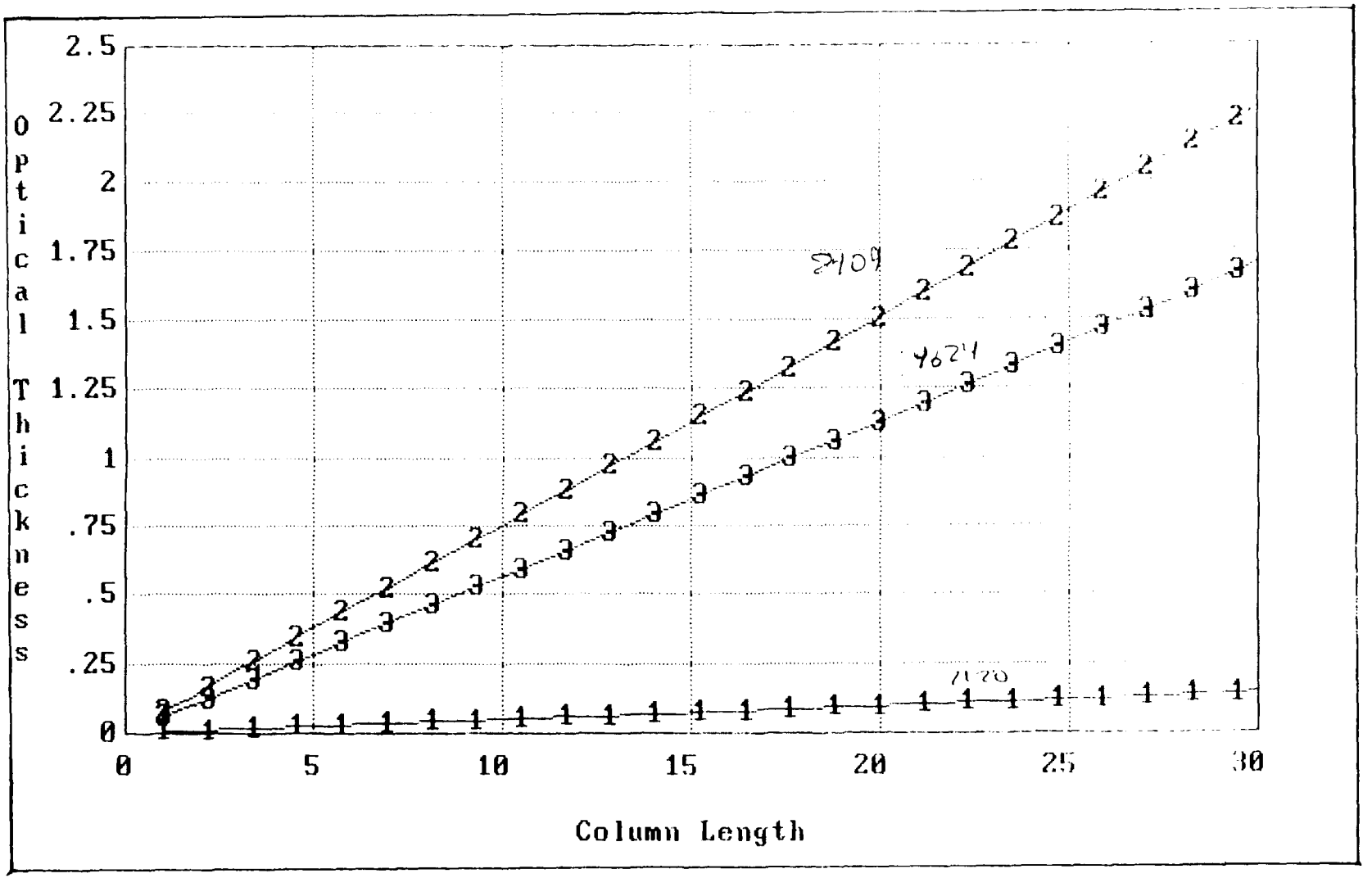

Figure 7: Dependence of optical Thickness upon Positive Column length for ne = 1E12. Same notation as figure 5.

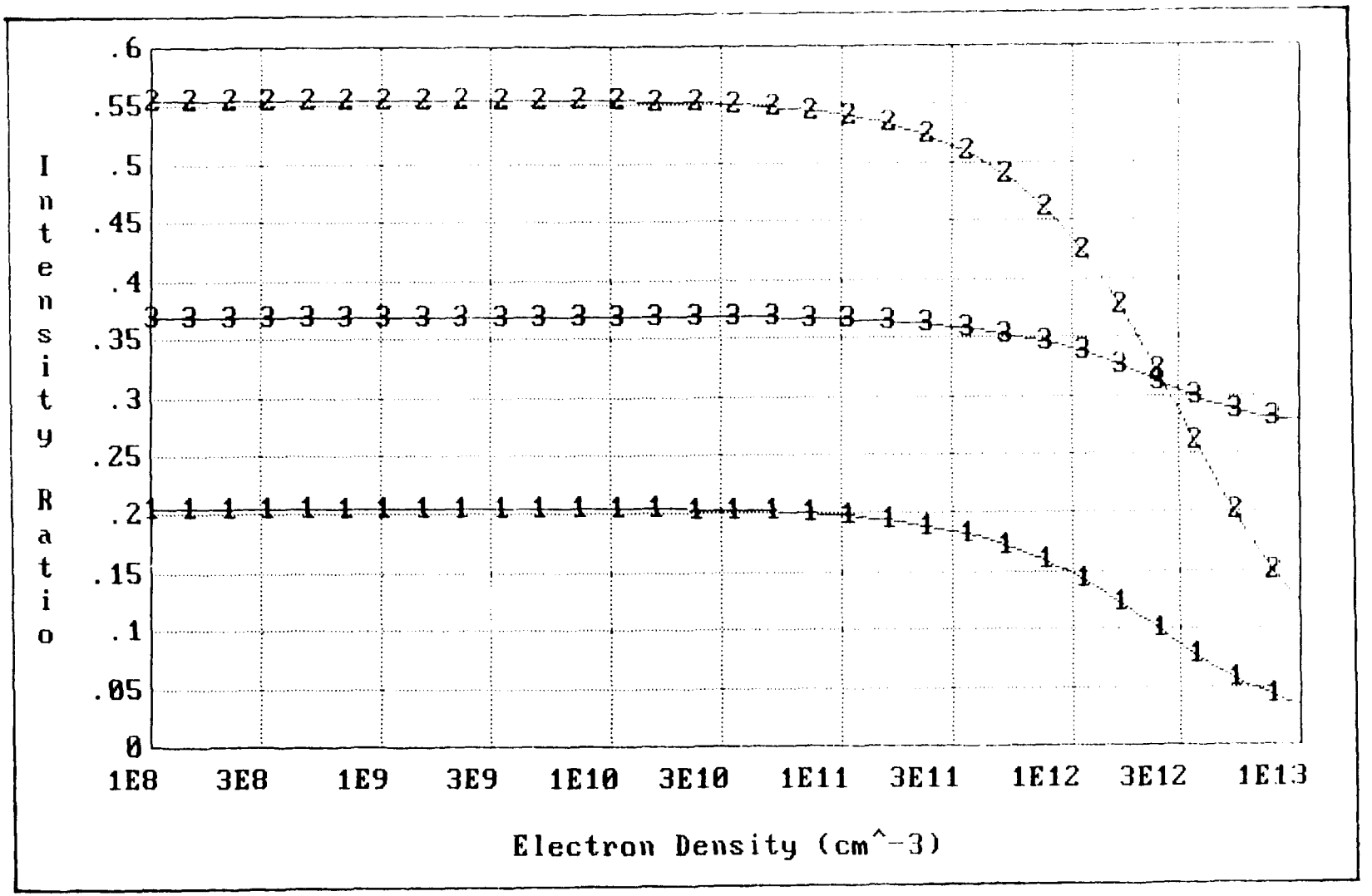

Figure 8: Intensity Ratio dependence on electron density for L =10cm

Discharge Oscillations

Many different types of discharge oscillations have been observed over the past century. These can vary in frequency from DC (standing striations) to GHz (electron plasma oscillations). Four types generally are prevalent[17] in the case of low-pressure rare gas discharges. These are; (1) relaxation oscillations, (2) electron plasma oscillations, (3) stationary striations, and (4) moving striations.

Relaxation Oscillations . Relaxation oscillations are, in actuality, circuit oscillations rather than discharge oscillations[18]. Relaxation oscillations are due primarily to the distributed capacitance of the discharge. In this case, the discharge itself acts as a capacitor that is continuously charged and discharged. This capacitor, coupled with the resistance of the circuit, acts as a switch, turning the circuit on and off for a period determined by the RC product. The discharge is then said to be intermittent and is considered unstable. Relaxation oscillations can quickly be ascertained by examining the relative phase shift between two separate points along the discharge column. Since these are circuit oscillations, the relative phase shift between any two points will be zero.

Electron Plasma Oscillations . Electron plasma oscillations are the result of the electrons oscillating about some mean position, and are generally found in all discharges. They are generally described in terms of a perturbation in the displacement of an electron under the influence of a constant electric field, but can also be described by the application of

Maxwell's equations, the force equation and the current flow equation[19]. The result is an expression for the plasma frequency,

$$f = \sqrt{\frac{ne^2}{\pi m}}\ , \tag{37}$$

where dispersion has been neglected. Electron densities for low-pressure discharges are typically on the order of 10^{10} cm^{-3}, resulting in a plasma frequency of about 10^9 Hz.

Striations. The other two types of oscillations to be discussed are stationary striations and moving striations. Both are part of a larger class of waves termed ionization waves, characterized by variations in the spatial and temporal ionization rates along the positive column of a discharge. Pekarek[20] has presented a theory whereby ionization waves are created by a small perturbation in the plasma density. Lee and Garscadden have elaborated on and refined this theory to explain both moving[21] and stationary[22] striations. In general, the perturbation in the plasma density creates local changes in the electric field brought about by the diffusion of charged particles. This variation in the electric field changes the local ionization rate which consequently changes the excited state densities. Briefly, Pekarek's equation of continuity for ion production is given as follows;

$$\frac{\partial n}{\partial t} = D_a\frac{\partial^2 n}{\partial z^2} + c_1 n - c_2\int_z^{\infty}\{\exp[-a_1(\varphi - z)]\}n(\varphi,t)d\varphi\ , \tag{38}$$

where

$$c_1 = Z_\theta^1 b_1 T_e\ ,\ \text{and}\ \ c_2 = Z_\theta^1 b_1[T_e a_1 + E_0]\ . \tag{39}$$

The first term represents the diffusion losses, the second term represents the ionization rate, and the third term is the perturbation term put forward by Pekarek, which represents the perturbation of the plasma density. Z_θ^1 is the derivative of the ionization rate with respect to the electron temperature θ , $b_1 \approx 3e/2$, a_1 is the reciprocal of the electron temperature relaxation length, and E_0 is the axial electric field. Solution of this equation is somewhat complicated and beyond the scope of this study, and the reader is referred to the original papers for a complete discussion. A brief review is given in the following sections.

Moving Striations . For moving striations, the ion density is assumed to have a Fourier series representation. The solution to Eq (38) is then dominated by an $\exp(-\Phi t)$ term, where the attenuation factor is given as

$$\Phi(\sigma) = D_a\sigma^2 - c_1 + c_2a_1/(a_1^2 + \sigma^2), \qquad (40)$$

where σ is the wave number of the oscillation. If $\Phi(\sigma) > 0$, then the disturbance is damped and no self-excited oscillations will occur. On the other hand, if $\Phi(\sigma) < 0$, then oscillations will occur and be sustained. In addition, if $\sigma^2 > a_1^2$, i. e., the striation wavelength is less than 2π times the relaxation length,then the wave will have a backward-wave nature. In low pressure discharges where ambipolar diffusion is operative, equation (40) is usually satisfied.

Stationary Striations . For stationary striations, the development of Eq (38) is modified somewhat to allow for a bounded system. This results in a second-order partial differential equation for the ion density. The

dispersion relation for this equation is given as

$$k^3 - ik^2 - ((\beta + i\omega)/\alpha)k + [\omega/\alpha + i(1 - \beta)/\alpha] = 0 , \qquad (41)$$

where

$$\alpha = a_1{}^3 D_a/c_2 , \text{ and } \beta = a_1 c_1/c_2 , \qquad (42)$$

and c1 and c2 are as before. For $\omega = 0$,

$$k^3 - ik^2 - (\beta/\alpha)k + [\, i(1 - \beta)/\alpha] = 0 , \qquad (43)$$

and the solutions are of the form U = exp(ikaz) where k is any root of the dispersion relation. The solution is dependent on the boundary conditions at hand and is somewhat complicated to solve, but forms the basis in which to model the standing striations.

The general result shows that three qualitative characteristics are associated with so-called normal modes of striations based on this theory: (1) The the striations will tend to be damped toward the anode, (2) the striations will be damped as pressure is increased, and (3) the wavelength of the striations do not vary with pressure. Again the reader is referred to Ref. [ ] for a detailed analysis of these statements.

Effects on Intensity Measurements

The two types of oscillations that will be examined in this study are moving and stationary striations. The primary reason is that these types of oscillations can have a significant impact upon the intensity of a spectral line and its interpretation. The variation in the spatial location of the striation as the current is changed may represent a significant error in the

interpretation of the excited state density variation. For example, a large decrease in the intensity of a spectral line at some particular current value may indicate that a large change in the ionization rate has occurred for that level. On the other hand, if stationary striations are present, the intensity change may indicated a change in the eigenmodes of the discharge, and are the result of a shift in striation location. In addition the time-dependent solution may require a different discharge voltage then the steady state solution, although at this time it is not known how this could change.

IV. Experimental Apparatus

Design / Layout

The experimental layout generally used is shown in figure 9. Three tubes were examined in the measurements. The first was a hot filament

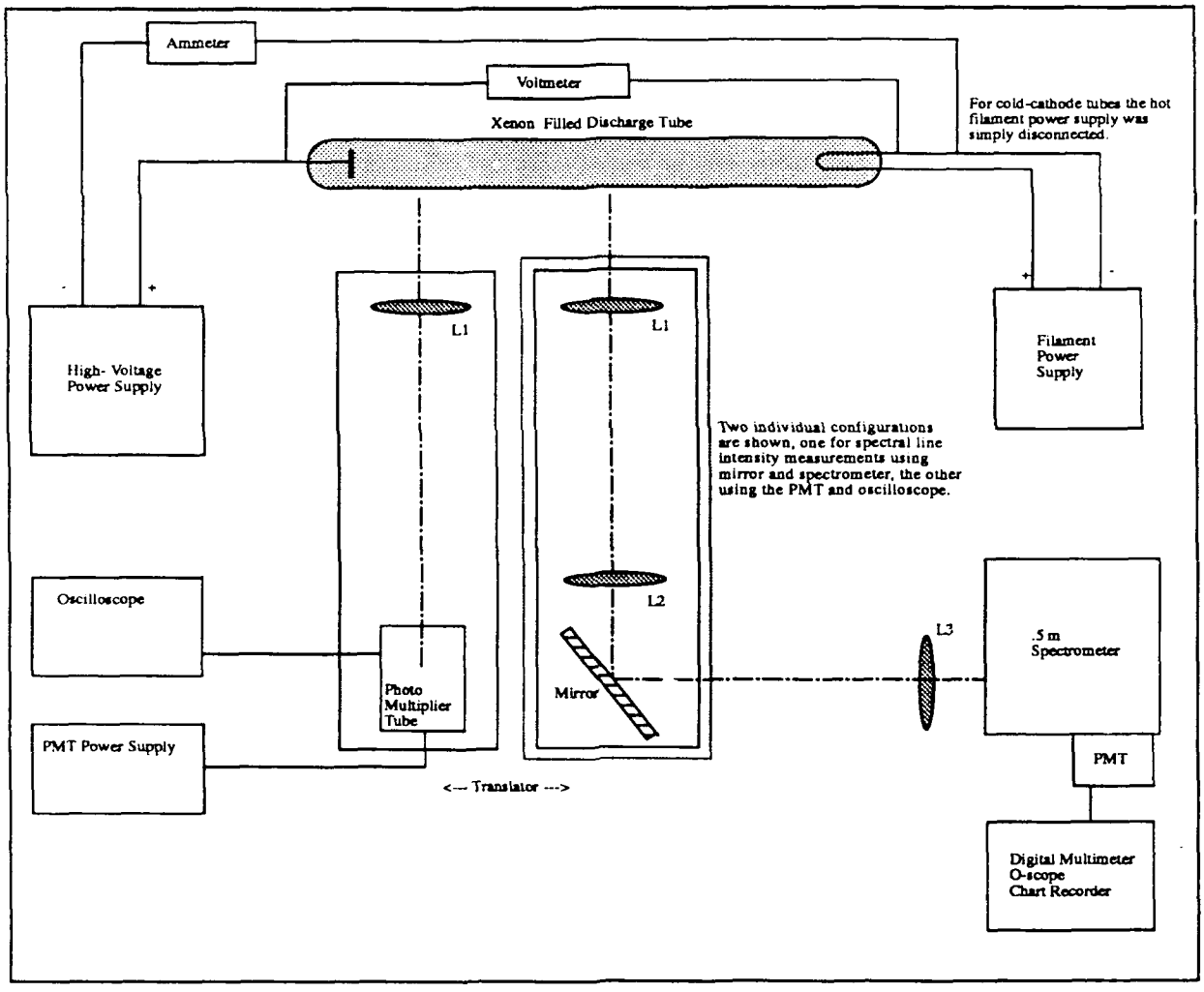

Figure 9 : Experimental Set-up

type tube approximately 90 cm long, with an inter-electrode distance of about 67 cm, and an inside radius of 1 cm. Electrodes consisted of a Thoriated Tungsten filament ribbon cathode and a hollow tube nickel anode approximately 1 cm in diameter and 5 cm long. Layout and mounting of the tube allowed a 40 cm section of the positive column to be observed. The second tube examined was a 30 cm long cold cathode tube, with an inside radius of about .3 cm. and both hollow-tube type nickel electrodes. Layout and mounting of this tube allowed for a 10 cm section of the positive column to be observed. The tube used for radiation trapping measurements was also of the cold cathode type. The electrodes for this tube were mounted perpendicular to the positive column in order to provide for observation along the tubes axis as well as radially. Tube length was 40 cm with an inner bore radius of 1 cm. Inter-electrode spacing was 30 cm. Quartz windows were mounted on the tube ends for axial viewing. Prior to use each tube was evacuated to less than 10^{-6} Torr. Each tube was outgassed either by filament heating, as in the hot filament case, or by induction heating, as in the cold cathode case. The tubes were then filled to the appropriate pressure of 99.995% pure Xenon gas and sealed.

Voltage -Current Measurement Equipment

Power supplies . Two power supplies were used in the experiment to provide power for the discharges. The first was an Aerospace Research Labs (now Wright Research and Development Center) current-controlled

high- voltage power supply which provided the supply voltage necessary to maintain the discharge. It provided up to 5kV of voltage and up to 100mA. Current control was provided for by a vacuum triode tube, which eliminated the necessity for a ballast resistor. The second power supply was a Kepco Model JQE 55-10 which provided the filament heating current for the hot filament tube. This supply could provide up to 55 V at 10 A if necessary but was normally operated at about 5-10A and about 5V, depending on the tube pressure. Measured ripple was <10mV p-p at 3.4V.

Meters . A digital voltmeter was used to measure the discharge voltage, and an analog meter was used to measure the discharge current. A Kiethley Model 177 digital multi-meter(DMM) was used to measure the discharge voltage. The specified error in voltage measurements for the meter was specified as ±.2% of the reading + 1 digit. A Fluke 80K - 40 High Voltage Probe was used in conjunction with the meter to provide high enough impedance so the circuit loading would not be a problem. The probe impedance was specified as 1GΩ, and the specified accuracy at 1kV was ± 4%. It was thought that the actual error might be better than 4% so the probe was measured against a recently calibrated meter at 1kV. The error turned out to be ± 1%.

Discharge current was measured with a Weston 911 analog ammeter, with ranges of 10mA to 10A. The specified error for the meter was specified as ± 2% for the 300mA range, but had not been calibrated recently. Therefore, the error in the reading was arbitrarily taken as ±5%.

Intensity Measurement Equipment

Optics . Two (10 and 15 cm focal length) uncoated lenses were used at the tube and at the slit entrance, to guide the light onto the spectrometer entrance slit. The lens at the tube end served to collimate the axial light while the lens at the slit end focused the light onto the tube. The use of the 45°mirror provided the means to measure the light intensity at any point along the column.

To eliminate confusion with 2nd order lines, a CS3-72 low pass filter was inserted just in front of the entrance slit. The wavelength transmission(>50%) range for the filter was 4600Å to 2.75 microns. In addition, for strong lines a #1 neutral density filter was inserted as needed to prevent photomultiplier tube(PMT) damage.

Spectrometer . Intensity measurements of individual spectral lines were made with a SPEX 1870 .5m Czerny-Turner Scanning spectrometer with a scanning range of 1750Å to 12800Å. The system was fitted with an 1872 Minidrive which provided for automated scanning at speeds of .01 to 5 Å/s, in addition to manual positioning. The spectrometer was specified as having a resolution of .25Å, accuracy of ±2Å over 5000Å, and a repeatability of ± .8Å. Wavelength separation was provided by a 1200 grooves/mm diffraction grating blazed at 5000Å. The slits were set to between 10 and 80 Å during the experiment. This resulted in wavelength resolution of about 1 to 2 Å (FWHM).

Photomultiplier Tube (PMT) . A cooled RCA type C31034 11 stage

Gallium Arsenide photomultiplier tube was mounted on the exit slit of the spectrometer to measure the light intensity of the spectral lines. The tube was kept at a temperature of -30°C to significantly reduce the noise level(35cps @-20°C typically), and also to provide measurements to 9300Å. The maximum allowed current through the tube was specified at 100nA,hence the necessity for the neutral density filter.

Meters. A Fluke Model 8200A DVM was used to measure the photomultiplier output current through a precision resistor. The meter has a specified error of ±(.02% of input + .02% of range) for the 10V range. The error of the 100mV range used was assumed to be similar and taken as ±(.1% of input + .1% of range). The accuracy of the resistor used was ±1%.

X-Y Recorder . Wavelength and axial scans, as well as line profiles were documented on an HP7090 X-Y Recorder. The X channel was time while the Y-channel measured the intensity from the photomultiplier tube. Again, a 1% resister was used to measure the intensity. In addition, a .5μF capacitor was placed across the input to limit noise oscillations($\tau = .5$ s). For wavelength scans, the recorder was triggered by a signal from the spectrometer scan drive. Typical scans were run at 1 Å/s, which implies a wavelength error of .5Å. For axial intensity measurements, the recorder was triggered by a limit switch mounted on the translator, which provided a consistent starting point (± .1 cm).

Oscilloscope . Intensity oscillations for individual spectral lines were measured in the same manner as normal intensity measurements, except that the PMT output was measured on a LeCroy dual channel 9400 oscillos-

cope. The scope has a specified bandwidth of 125MHz. In addition, the scope includes a Fast-Fourier Transform(FFT) section which provided for frequency measurements of the intensity oscillations. Accuracy is specified as ±2%. Input impedance chosen was1MΩ.

V. Experimental Procedure

Discharge Start-up and Operation. For the hot filament tube, the discharge was started by adjusting the hot filament current to a predetermined level. This current was initially determined by measuring the filament temperature with a pyrometer, and adjusting the current until the filament temperature was approximately 1800°C. Typical filament current and voltage readings for the tube were 4.6A and 3.4V at 1 Torr and 5.8A and 5V at 10 Torr. The high voltage supply was set to approximately 1.5kV. This setting provided enough voltage to sustain the discharge at the low currents yet not overload the power supply at the higher currents. At the higher currents the triode tube in the power supply would overheat if the supply voltage was to high. Current was varied by the current control potentiometer on the power supply.

For the cold cathode tubes, the voltage was increased until breakdown occurred for the 1 Torr case. In the 10 Torr tube starting was assisted by a Tesla RF coil, while the supply voltage was set to 3kV. A common reference supply voltage was 2kV at 1mA for the 1 Torr tube and 3kV at 1mA for the 10 Torr tube. Once this initial setting was made, the current was reduced to the starting current for the intensity measurements.

Intensity Measurement . Once the discharge was started, the current was set to the starting point (typically about .4mA) and allowed to settle for at least 5 minutes. The current was controlled at the high voltage power

supply while monitoring the ammeter connected in series with the discharge. Intensity was measured directly from the DMM connected to the PMT output. Five readings of the intensity were taken for each current setting, and a waiting period of at least 2-3 min. was allowed after each current setting to allow the discharge temperature to stabilize.

An initial survey of 17 different transitions were examined initially to determine if any anomalies existed. Four representative transitions were then selected for further examination. These lines are listed as follows:

Wavelength (Å)	Transition
4624	$7p[3/2]_2$ - $6s[3/2]_2$
7120	$7d[7/2]_4$ - $6p[5/2]_3$
7968	$7p[3/2]_1$ - $6s'[1/2]_0$
8409	$6p[3/2]_1$ - $6s[3/2]_2$

The intensity of these four lines was measured for currents typically from .1 to 40 mA. The exact range depended on the tube and pressure. The lower limit was generally governed by the ability to sustain a discharge, while the upper end was limited by cathode heating.

Voltage Measurement . The discharge voltage was measured in conjunction with the intensity measurements. At each current setting, the voltage was read directly from the DMM connected across the discharge. Only one reading of discharge voltage was made for each current setting. A total of four separate readings were obtained since four individual intensity measurements(4 lines) were made. This measurement was made for each

of the four tube configurations.

Oscillations . Moving striations were measured by observing the photomultiplier output on the oscilloscope. The oscillation peak and frequency of the 4624Å line was measured for the cold cathode tube at 10 Torr. To measure the oscillation peak, the trigger level was increased until no oscillations were observed, the decreased until a constant number of oscillations was observed, i. e. the trigger light stayed on. This point was arbitrarily set as the peak of the waveform(t=0). The peak intensity for an average of 500 waveforms was then recorded. The timebase was typically short (.1 ms) for this measurement to provide better waveform resolution.

A similar set-up was used to measure oscillation frequency. The difference was that the timebase was fairly long (~ 10 ms) in this case for better frequency resolution. The oscillation frequency was determined using the FFT option on the oscilloscope, again for an average of 500 waveforms.

Standing Striations . The intensity of standing striations was measured for the cold cathode tube at both 1 and 10 Torr. The PMT output was connected to the X-Y recorder for this measurement. Only the 8409Å line was measured. The recording was triggered by a limit switch mounted on the translator. The translator speed was set so that the distance between the anode and cathode (d ≈ 15 cm) could be observed in a 2 minute scan period.

Radiation Trapping . Radiation trapping was measured on the axial tube described in the previous section. This tube allowed measurement of the radial and axial intensity(not simultaneously). The radial intensity was measured in the standard way described in the intensity measurement section, although only a current of 4 was measured. To measure the axial intensity the tube was rotated and positioned so that the end of the tube observed was at the radial position observed before. In both cases the lens at the tube end (L1) was removed so that a collimated section of the tube was observed.

Calibration . The intensity measuring system was calibrated in order to provide further information to be used at a later time(i.e. Te determination). A calibrated standard lamp was placed at the tube location to provide broadband illumination. The slit was set to 10 microns x .2 cm and the intensity recorded for a scan from 4500 to 9000Å. Two calibration runs were made for this system; one without the neutral density filter installed, and one without. In addition, the intensity variation with respect to slit width and height were also recorded.

VI. Results and Discussion

Intensity Measurements and Voltage - Current Characteristics

The results of the intensity measurements and the V-I characteristics will be presented together for each case. The hot filament tube will be discussed first, for each pressure, followed by a discussion of the cold cathode tube.

Hot Filament Tube at 1 Torr. The V-I characteristic for the hot filament tube at 1 Torr is shown in figure 10. The discharge voltage decreased from about 130V to approximately 60V. Assuming that the cathode fall voltage(V_c) is constant over this range, then the voltage variation observed would be due entirely to changes in the positive column. The length of the column was found to be approximately 60 ± 2 cm long. Assuming the minimum value of V_c is about twice the ionization potential of Xenon, then the maximum electric field within the column varied between 1.8 and 6 V/cm. For a fixed pressure ($N \approx 3 \times 10^{16}$ cm^{-3}), then this implies a decrease in the E/N, and consequently the electron temperature. A decrease in E/N could possibly be explained by two mechanisms.

The first is increased influence of stepwise excitation mechanisms. On the basis of Eq. (21), repeated below

$$D_a(2.405/R)2 = N_g R_{oi} + N_m R_{mi} + N_e R_{ei}\,, \qquad (21)$$

E/N must decrease in order to maintain the relatively constant diffusion balance as stepwise ionization mechanisms become more important. When single step ionization is dominant, Te and consequently E/N is

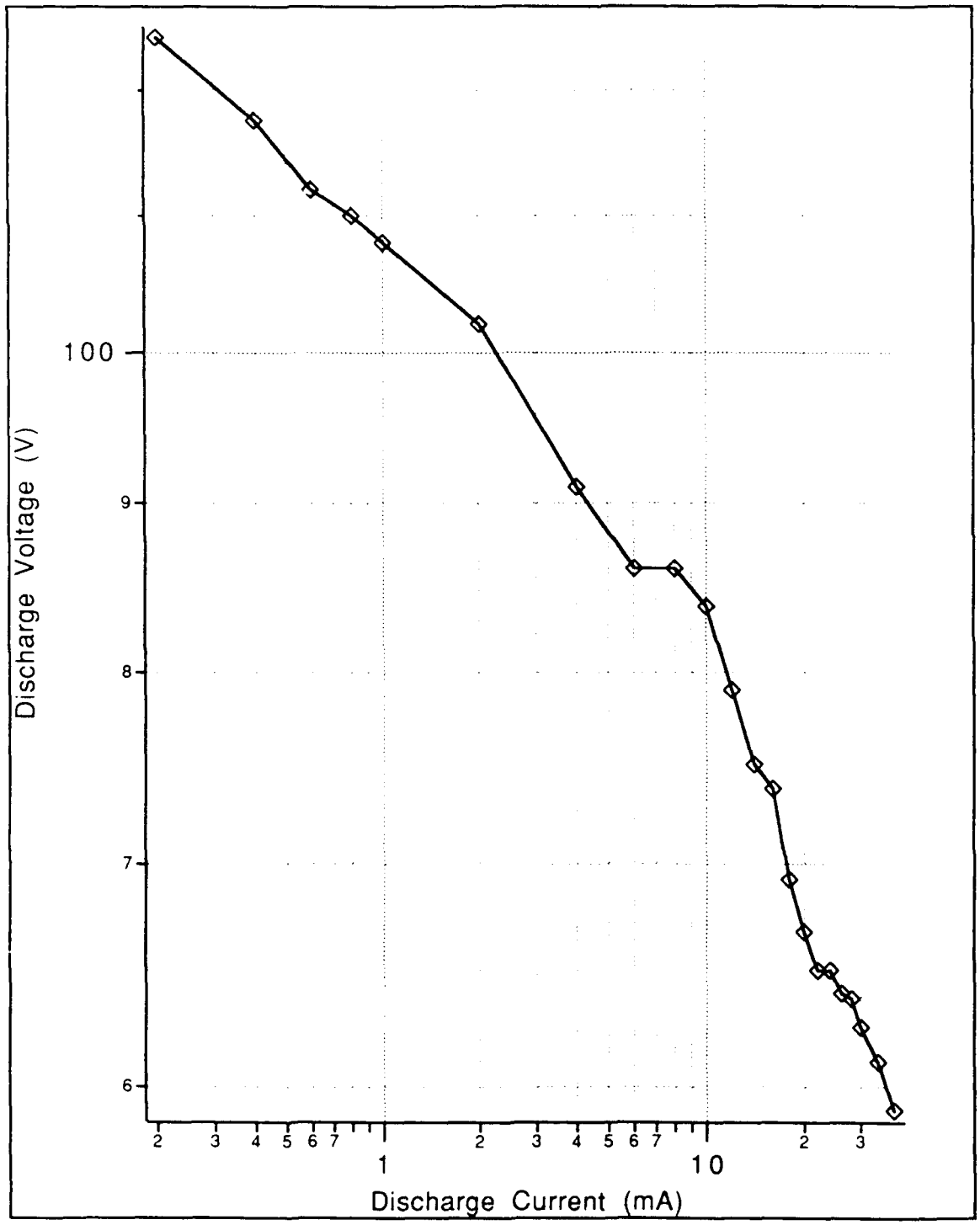

Figure 10: Voltage-Current Characteristic. Hot Filament Tube @ 1 Torr

prescribed by the PR product of the tube, as described before. As stepwise mechanisms become important, then all the terms must still maintain the same total ionization rate in order to maintain the balance between ionization and diffusion. The only way for this to be accomplished is to reduce the rate of single step ionization, which is then made up by the inclusion of the stepwise ionization terms in Eq (21). Since the rate coefficient is dependent upon the characteristic energy (T_e), then T_e must decrease, and therefore E/N must decrease.

The other way for a decreasing field to occur is through gas heating. The radial gas temperature profile in a glow discharge tube can be approximated by a parabolic profile with a maximum temperature at the centerline and decreasing to some wall temperature governed by heat conduction from the wall to ambient air. In order to maintain a constant pressure in the tube, the gas density must be a minimum value at the center of the tube and a maximum at the walls, the product of the number density and temperature being constant everywhere within the tube. This reduction in the center of the tube results in an increase in E/N. But in order to maintain the balance between diffusion and ionization, E/N must not change. Therefore the electric field in the column must decrease. In this case, since the change in discharge voltage was assumed to be due entirely to changes in the positive column voltage, the density must have decreased by a factor of two, which in turn means that the axial gas temperature increased by a factor of two. Since the gas temperature was not measured for this case, it is not certain whether or not this actually

occurred. It may be that the decreasing field was due to a combination of two effects, the first being the increased influence of step-wise ionization mechanisms, and the second being gas heating, either by elastic collisions within the gas or heating by the filament (~1800°C).

The intensity dependence on current is shown in figure 11. The figures show primarily a linear dependence, with a slightly stronger dependence in the region of 4 - 6 mA. The linear dependence could be explained by both single-step and step-wise mechanisms, depending on the exact gain and loss mechanisms at work in each level. At the higher currents, the intensity begins to level off. Decreasing intensity could be caused by either domination of the electron impact excitation mechanisms at the higher currents, or radiation trapping. As the electron-impact mechanisms become dominant over all others due to the increased electron densities, the state densities would become independent of current. This would tend to affect all the transitions though, with the magnitude of the effect being determined by the ratio of the rate coefficients.

In addition, if gas heating were occurring in the discharge, then this would also affect the intensity. Gas heating as stated before, would tend to decrease the neutral atom density on the axis of the tube. This in turn may cause a decrease in spectral line intensity since the excited state density is proportional to the ground state density, provided the rate coefficients are not changing. On the other hand as current is increasing, the electron density is increasing, so it is likely that the decrease in the neutral number density is compensated for by the increase in electron density. The net

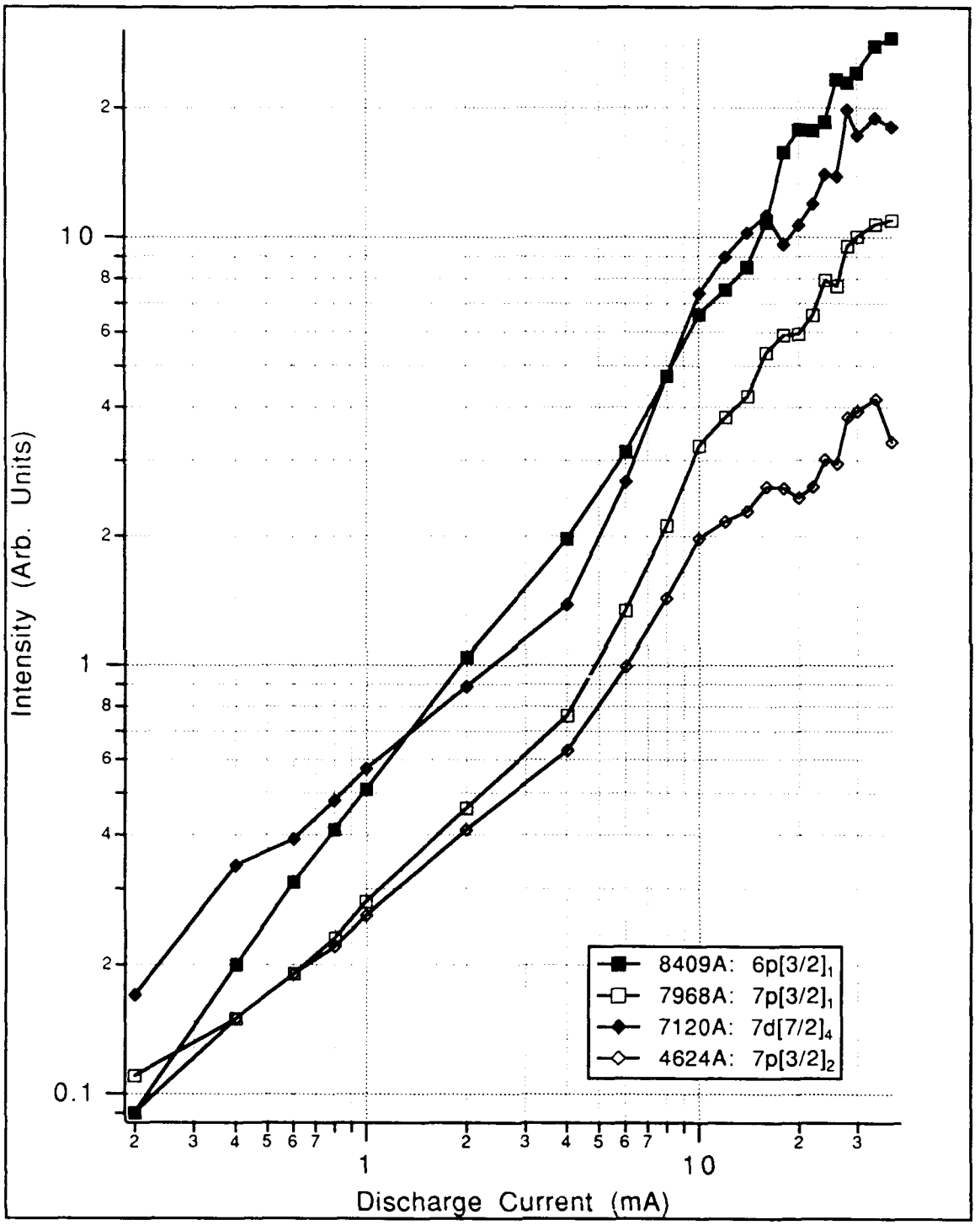

Figure 11: Intensity Dependence of Spectral Lines on Discharge Current. Hot Filament Tube @ 1 Torr

effect, then, may be that the intensity would not increase as fast as it would if gas heating were absent.

Radiation trapping may also be playing a role, but it is unlikely in this case, since radiation trapping would tend not to affect the 7120Å line since it does not terminate on a metastable, as shown in the background section. Therefore radiation trapping effects, if significant, would be evident by a decreased intensity of the lines which terminate on the metastable, and would not be evident on the line which did not terminate on the metastable (7120Å). Since the decrease in intensity occurred on all of the lines, including the 7120Å, then this must not be the result of radiation trapping.

Hot Filament Tube at 10 Torr. The observed characteristics for the hot filament tube at 10 Torr are shown in Figures 12 and 13. Two very interesting effects were noted for this case. First, the voltage increased for currents below .8 mA, from 500V to 720V , and then decreased by 600V over a current range from 1 to 40 mA. Secondly, when the current was increased from 4 to 6 mA, the intensity of the 8409Å transition suddenly decreased to about one-quarter of its 4 mA value. This effect was not noted in any of the other lines. This region is interesting because two other effects were noted. First, between 4 and 6 mA is the region where the discharge goes from a diffuse mode to a constricted mode, that is, the observed radius of the glowing column decreases by about one-half. In addition, the voltage level at 4 mA oscillates wildly up to ± 50V about a 300V mean value, whereas at the other currents the discharge voltage only oscillated by about 2V about the recorded value.

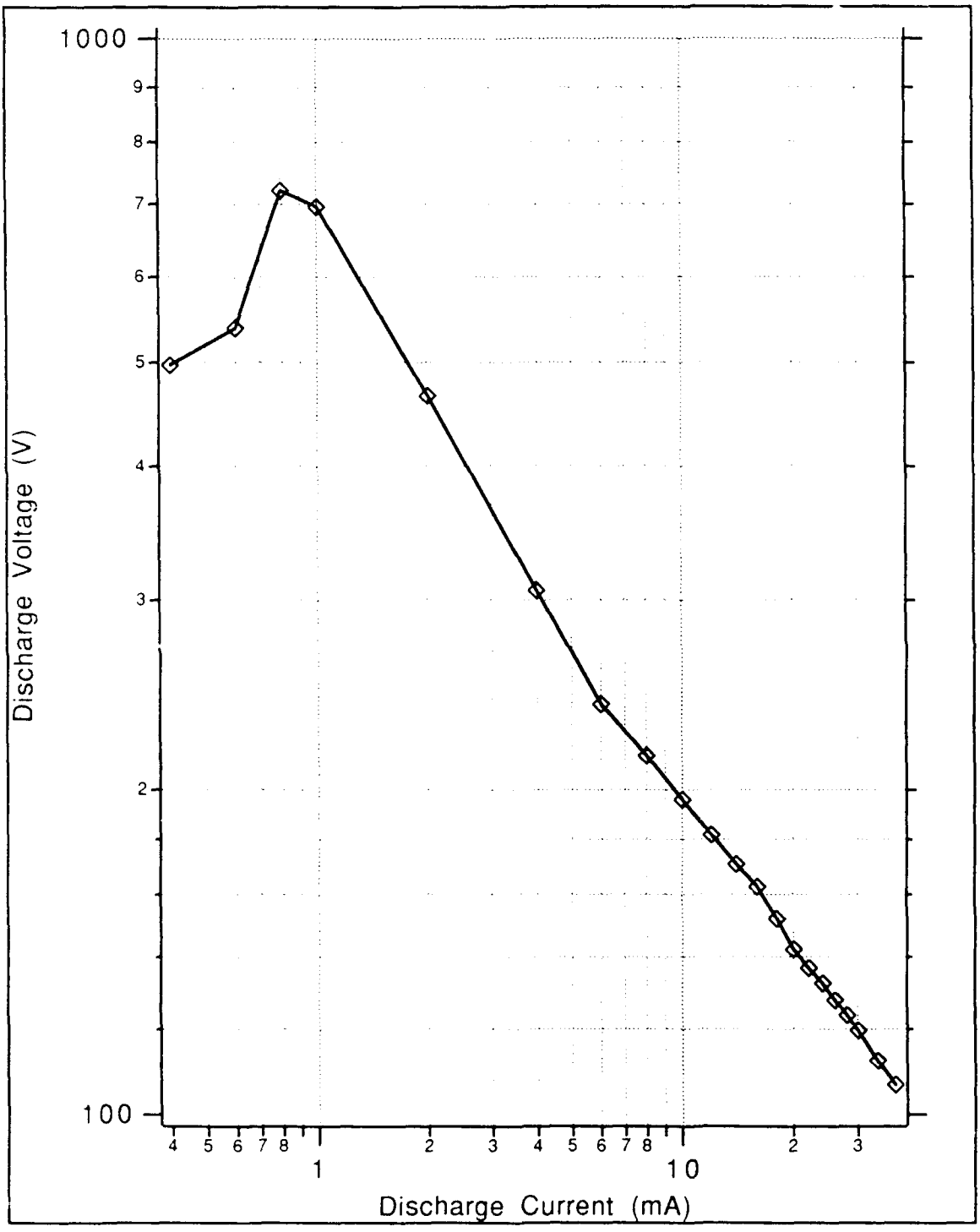

Figure 12: Voltage-Current Characteristic. Hot Filament Tube @10 Torr

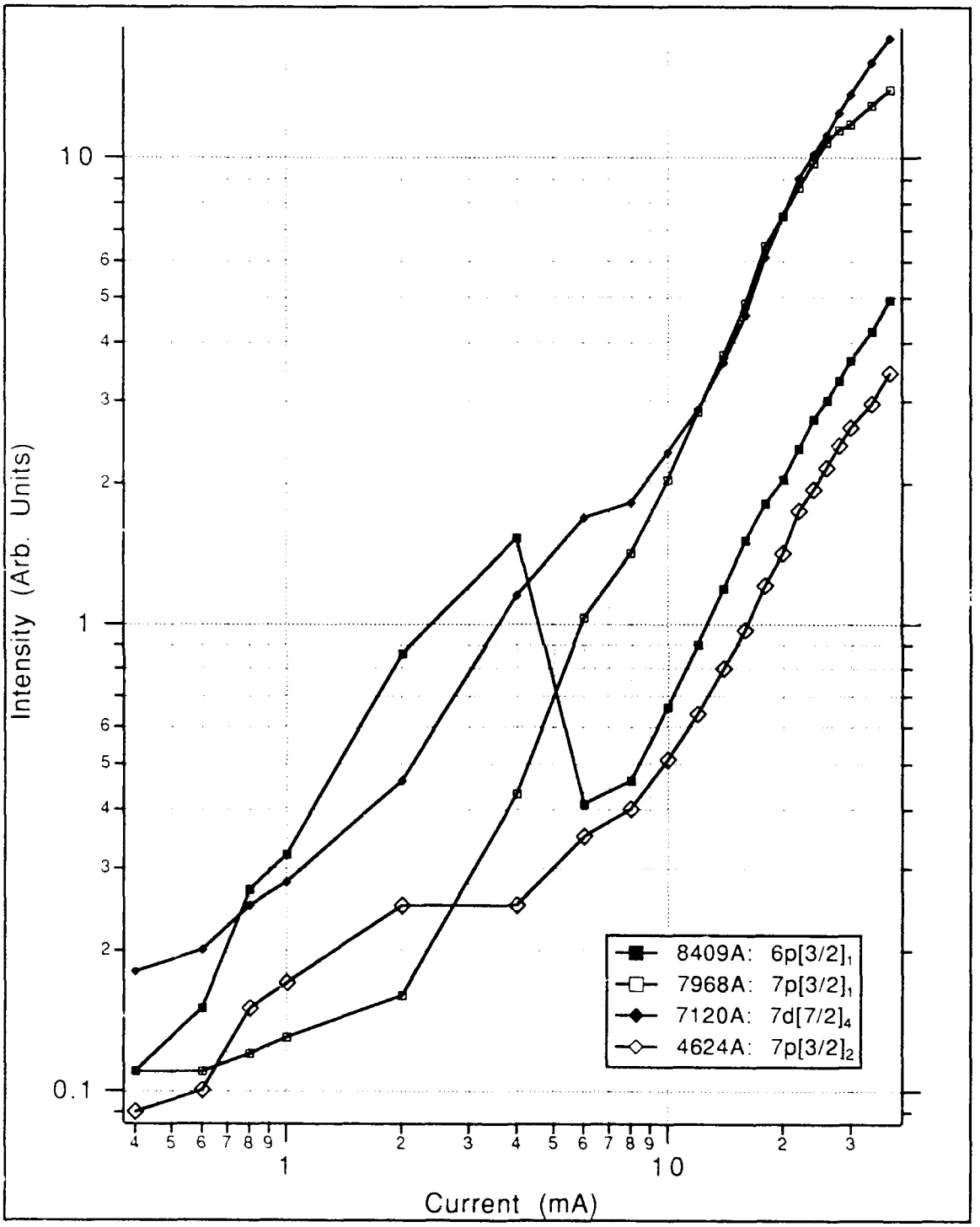

Figure 13: Intensity Dependence upon Discharge Current.
Hot Filament Tube @ 10 Torr

The factor of 7 increase in discharge voltage observed for the low currents in the 10 Torr case as compared to the 1 Torr case can be explained by diffusion balance arguments. First, referring to Figure 2 of the background section, one can see that as the PR product changes from 1 to 10 cm-Torr, the electron temperature only decreases from about .9 to .7 eV. This slight difference in T_e means that the corresponding E/N must not change very much either, since it is directly proportional to T_e. In order to maintain a constant E/N, the electric field must increase by a factor of 10 also, to compensate for the increase in N by a factor of 10. It is unlikely that the cathode fall voltage has changed much since it has been shown to be independent of pressure, for a constant E/N[23]. Therefore, just on the basis of these arguments, when the pressure in the discharge is increased from 1 to 10 Torr, it would be expected that the voltage would increase by a factor of around 10.

It is not clear why the discharge voltage decreases from 720 V to about 120V. It is unlikely that gas heating is responsible since a sevenfold decrease in voltage would imply a sixfold increase in axial gas temperature, which, if the gas temperature at the low currents was about 400K, then the gas temperature at 40mA would be about 2400K! It was decided to measure the wall temperatures of the tube at 10 Torr and 30 mA, to see if significant heating effects could be detected. The wall temperature at the filament was about 100°C while the wall temperature at the cathode end and anode end of the positive column were 40°C and 30°C, respectively. Following the analysis of Kosoruchkina[24] and using experimental data for

the positive column of Helium[25] and scaling the mass and thermal conductivities, it was estimated that for a wall of 300°K, the axial temperature for Xenon would be about 400°K. On the basis of this then, it is evident that some gas heating by the hot filament is occurring, but not enough to account for the large drop in the discharge voltage.

On the other hand, some significant gas heating may be occurring in connection with the contraction mechanism. Since the radius of the visible glow of the discharge decreased by a factor of 2 when contraction occurred, then it is likely that the electrons are more concentrated in the center of the tube. Since the electrons in the tube are primarily of low energy (~ 1eV), then most of their energy will be used in elastic collisions, i.e. gas heating. Therefore, it is possible that the axial gas temperature is somewhat hotter than expected. This would correspond to a large drop in the neutral number density on the discharge axis and a subsequent large drop in the electric field.

In addition, Bychkov[26] has reported that contraction in an inert gas argon discharge at pressures of 20 and 50 Torr is coincident with the formation of molecular argon ions, whose volume recombination coefficient is high, compared with their atomic counterparts. He has also shown that the number of molecular ions present is largely dependent upon the gas temperature, in essence, the hotter the region is then the less molecular ions there are. In this discharge then, the regions outside the visible glow would likely be the regions where volume recombination is high, whereas the region within the visible glow, i.e. the hot region, the recombination

rate would be somewhat lower. This would result in a discharge where both diffusion and recombination is occurring, and whose rates are varying with the electron density profile. It is not clear what the net effect of the combined diffusion-recombination mechanisms is on the discharge voltage. Generally, since recombination represents another electron loss mechanism, in addition to diffusion, then the rate of ionization must also increase. This would correspond to an increase in the electron temperature and consequently the electric field. It would be expected then, that the discharge voltage would actually increase, rather than decrease as observed.

The decrease in the intensity of the 8409Å line could possibly be explained in terms of the contraction mechanism also. If a large number of Xenon molecular ions are being formed in this discharge then it is possible that the 6p levels are being quenched by these. This may be because the energy of the 6p levels of atomic Xenon coincide with potential wells of several molecular levels[27] of Xe_2^+. Since the remaining levels corresponding to the other transitions are coincident with a much smaller number of molecular Xenon levels, then they would not be affected as much.

Cold Cathode Tube at 1 Torr. Figures 14 and 15 show the results of the measurements at 1 Torr. The V-I characteristics show a steady increase up to about 450V and then levels off. This is probably related to the onset of abnormal cathode glow that begins at about 2 mA. Abnormal cathode glow occurs when the area of the cathode is completely covered by the cathode glow. In the normal glow discharge the cathode fall voltage remained

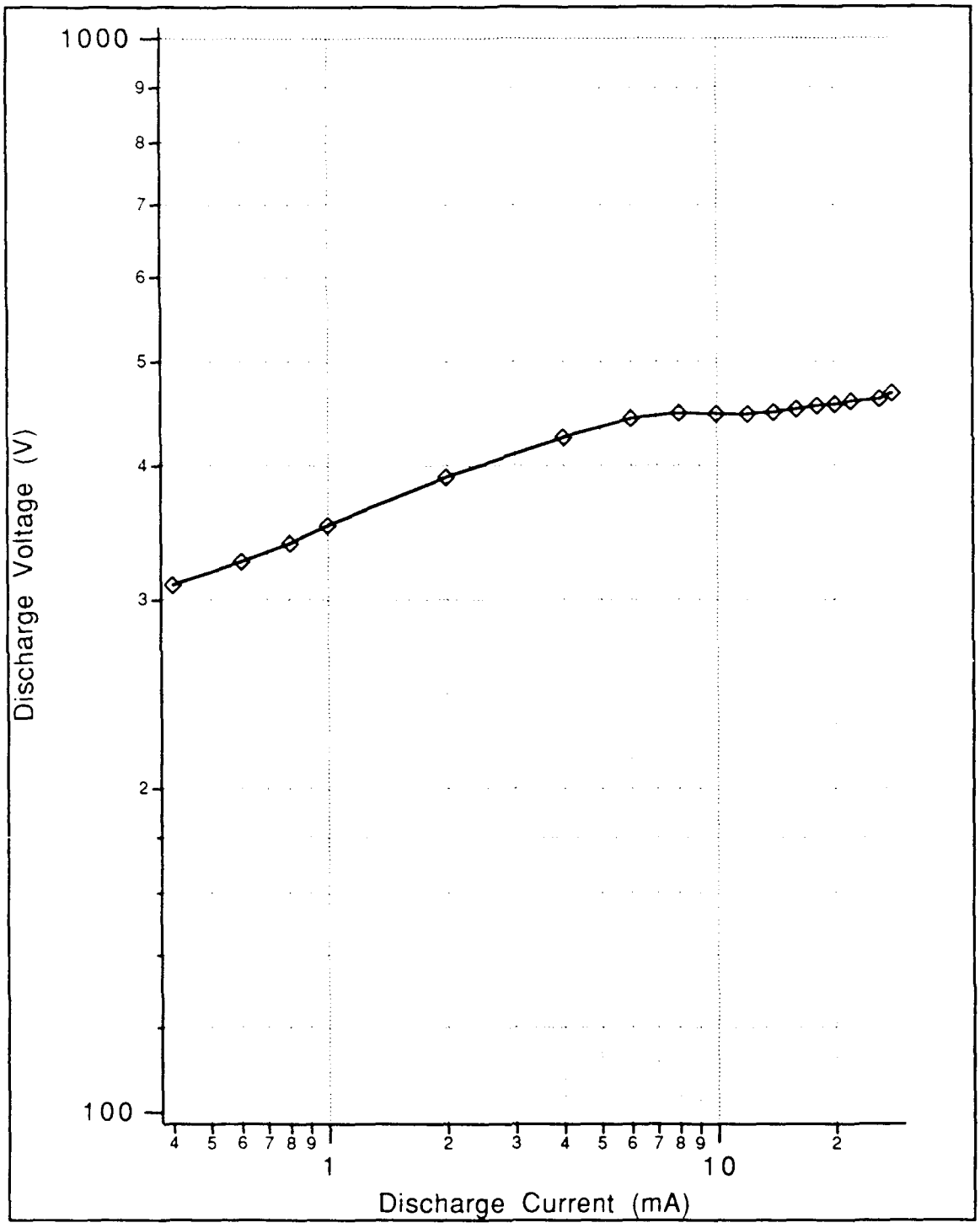

Figure 14: Voltage-Current Characteristic. Cold Cathode Tube @ 1 Torr

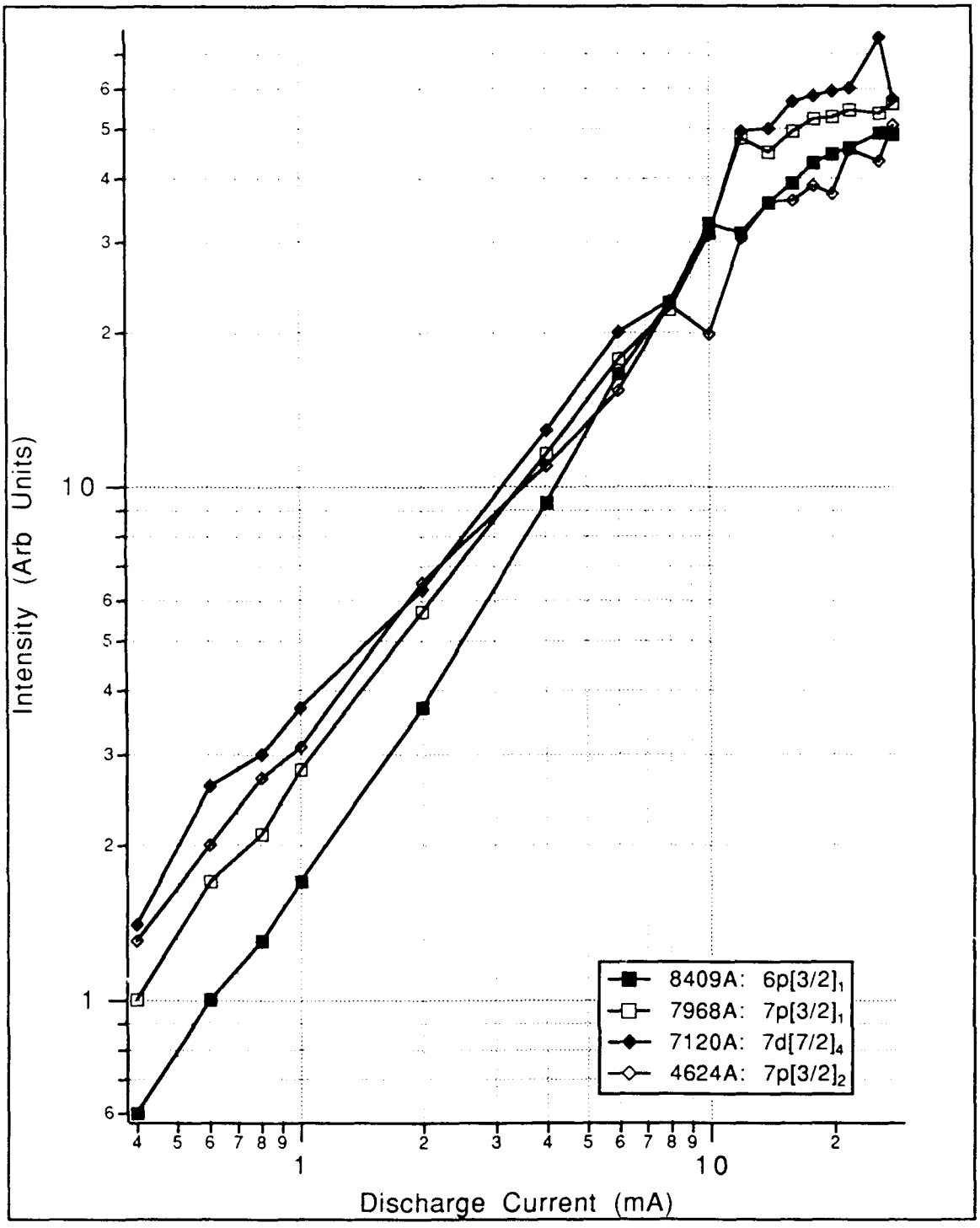

Figure 15: Intensity Dependence upon Current for Selected Transitions Cold Cathode Tube @ 1 Torr

constant because the current density remains constant; increased current simply increases the area of the glow. At the point where the cathode is completely covered, any further increase in current must be accompanied by a similar increase in current density and cathode fall voltage. Assuming then that the cathode fall voltage is responsible for the observed increase, then the positive column voltage is relatively constant. This condition could be the result of single-step mechanisms dominating ionization, thereby making the characteristic energy independent of current.

The intensity variation as current increased was primarily linear for increasing current, and leveling off at the higher currents(> 10 mA). The linear variation would tend to substantiate the case for single-step domination, although it may be possible to have stepwise mechanisms and still maintain a linear current dependence because of the complex interdependencies of the state densities. The tapering off at the upper currents is again probably due to saturation of the stepwise mechanisms since all lines are affected equally. It is not known why the 4624Å suddenly decreased at a current of 10 mA.

Cold Cathode Tube at 10 Torr. The cold cathode tube at 10 Torr also showed the onset of abnormal glow. In this case it began at about 20 mA. The increase in the V-I characteristic shown in figure 16 possibly reflects this onset. It is interesting however, that the voltage starts to increase before the visible occurrence of abnormal glow. In addition, the voltage observed at the low currents in the 10 Torr case is not much different than

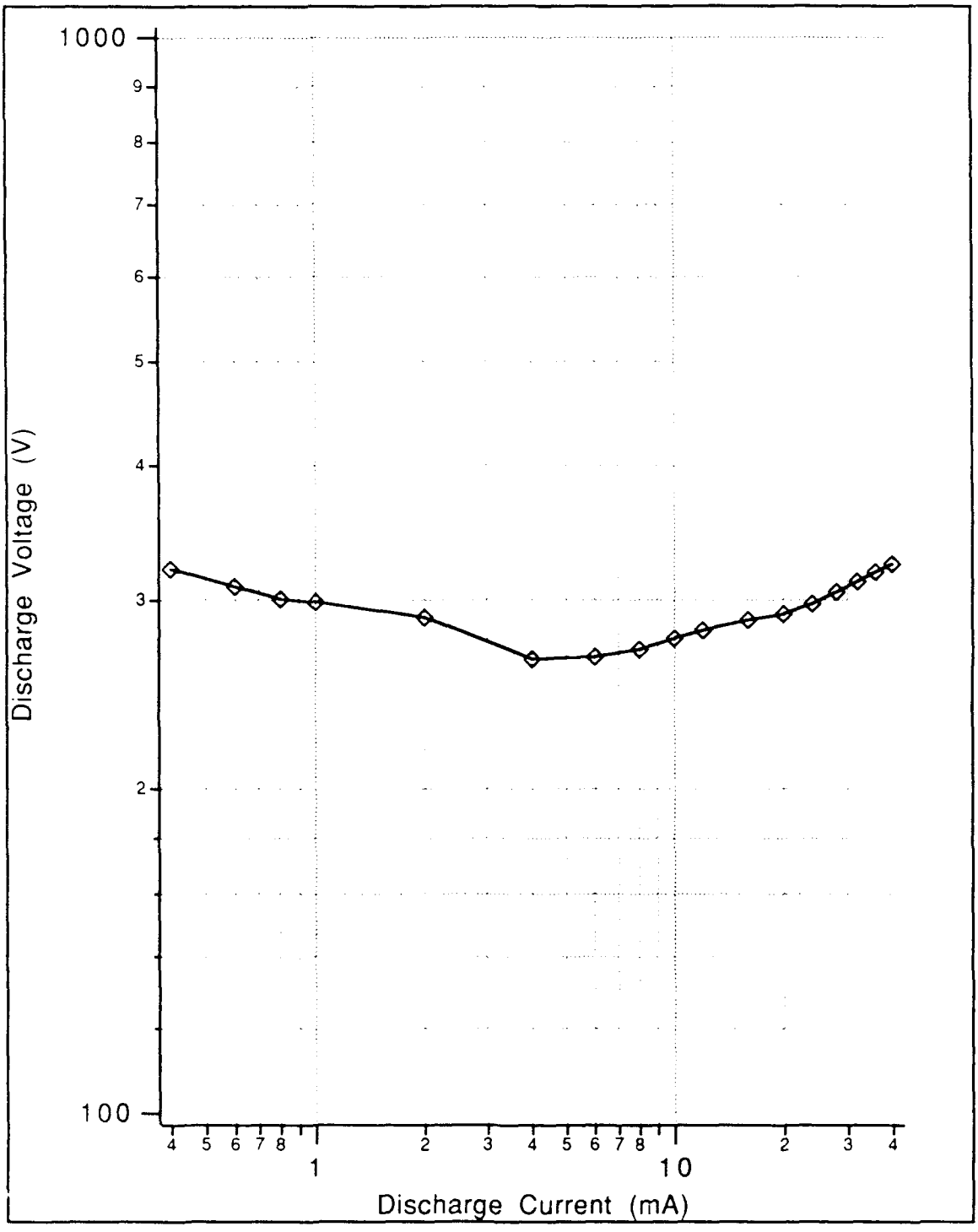

Figure 16: Voltage-Current Characteristics. Cold Cathode Tube @ 10 Torr

the corresponding voltage at 1 Torr. This is unusual since, as shown for the hot filament tube, if the pressure is increased by 10 Torr, then one would expect a 10-fold increase in the electric field, and subsequently the discharge voltage.

Figure 17 shows the intensity current relationship for this case. The intensity dependence upon current is primarily linear with a decreasing dependence at the higher currents. The linear dependence indicates that single-step mechanisms may be dominant. The decreasing influence of the current at the higher currents may be due to gas heating An increasing gas temperature would decrease the axial number density and subsequently the rate of increase of the intensity.

Standing Striations . Standing striations occurred intermittently in all the tubes, but their presence depended upon the current. Striation location location and amplitude were recorded for the cold cathode tube at both 1 and 10 Torr. The magnitude of the striations were much stronger for the 1 Torr case than for 10 Torr. At 10 Torr, the striation amplitude accounted for a maximum variation of about ±10% of the mean intensity along the column, and only occurred for currents of .8 and 1 mA. Figures 18 through 22 show the axial variation in intensity for the 1 Torr case. In this case, the intensity variation approached ±30%. The large peak observable at the cathode end is the negative glow discussed in the background section. The striation width ranged from .8 to 1.2 cm with no dependence upon current noted. Figure 23 shows how the intensity can vary in the positive column at two different

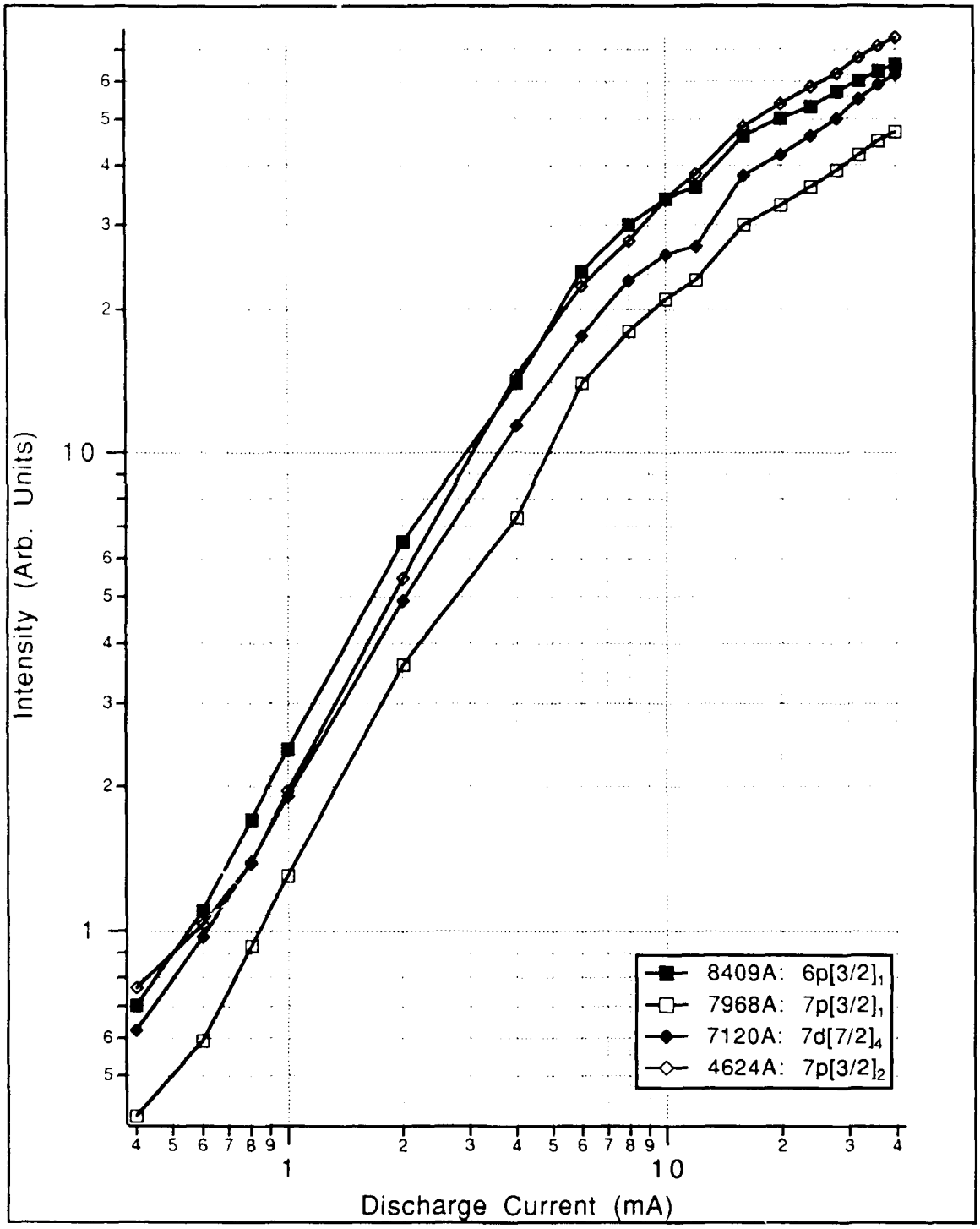

Figure 17: Intensity of Selected Transitions Upon Current
Cold Cathode Tube @ 10 Torr

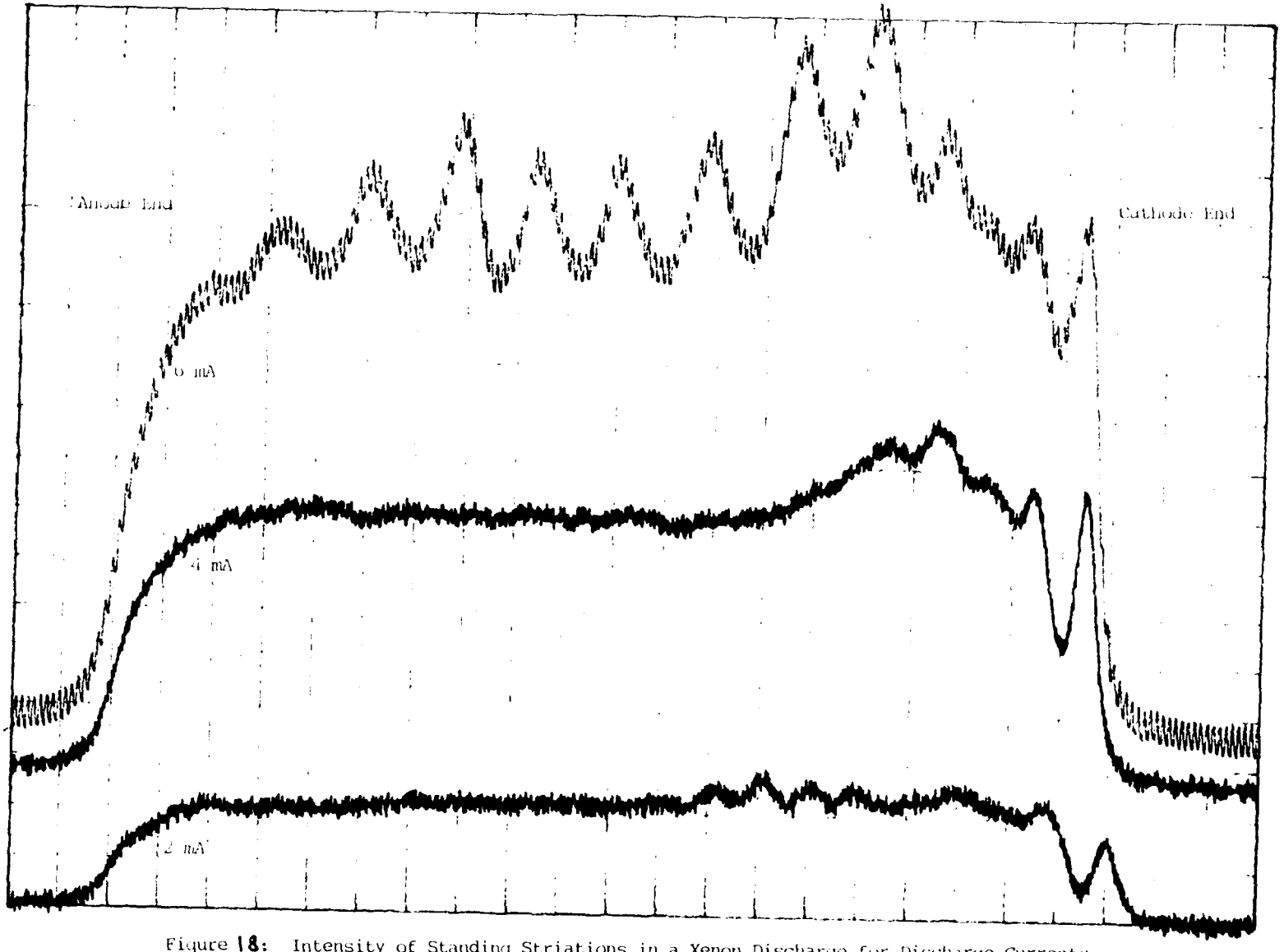

Figure 18: Intensity of Standing Striations in a Xenon Discharge for Discharge Currents of 2, 4, and 6 mA.

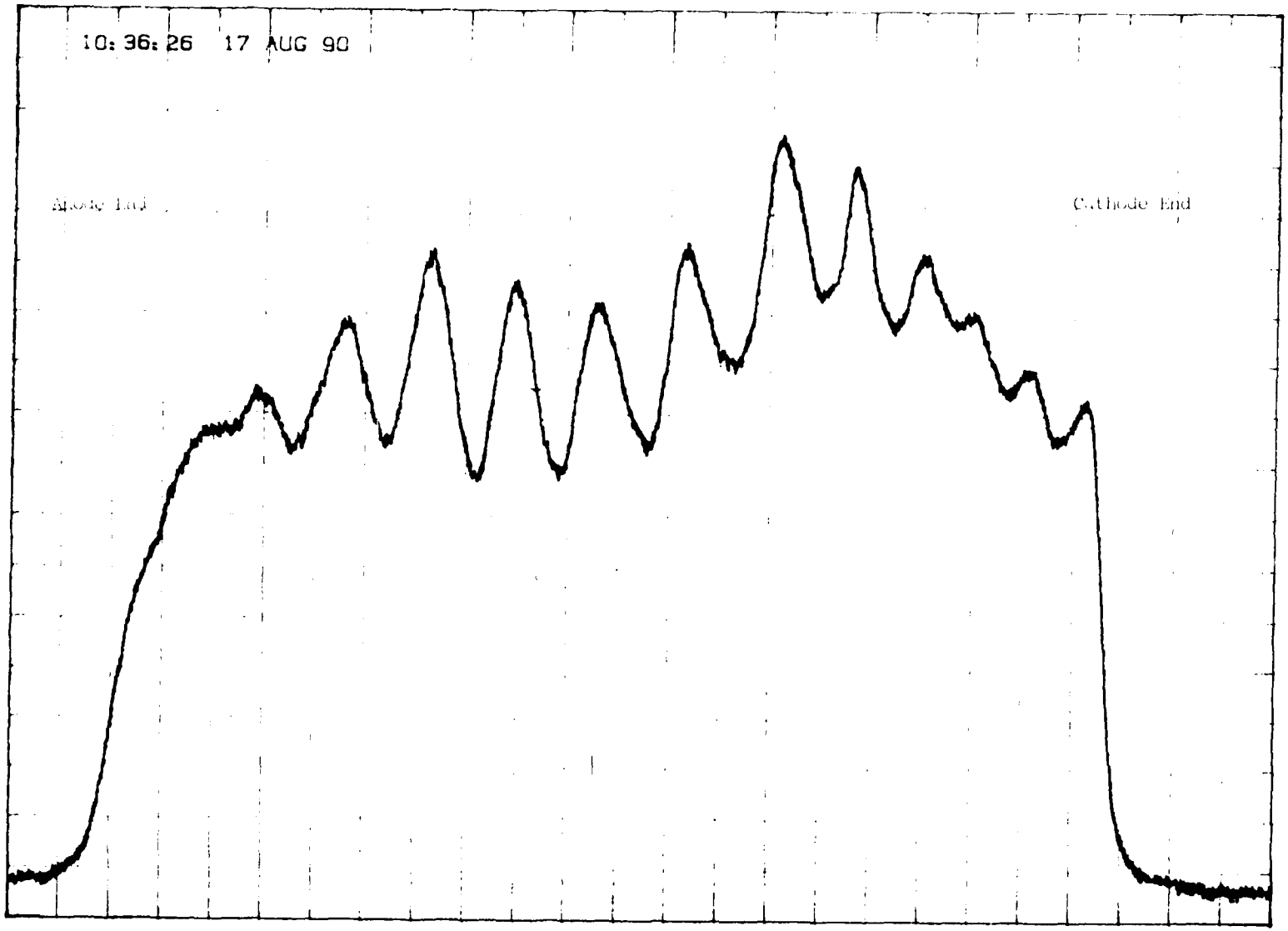

Figure 19: Intensity of Standing Striations in a Xenon Discharge for Discharge Currents of 8 mA.

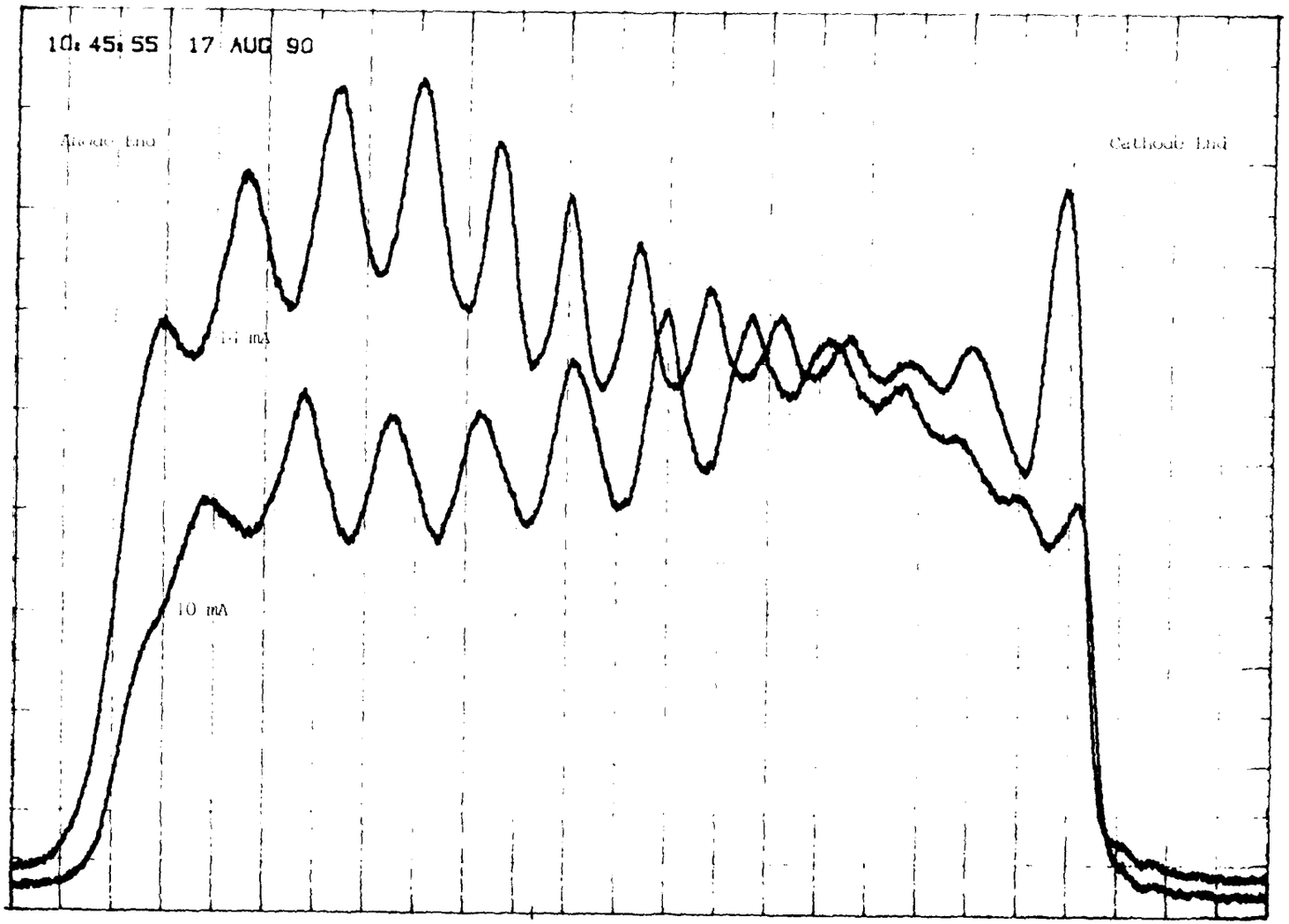

Figure 20: Intensity of Standing Striations in a Xenon Discharge for Discharge Currents of 10 and14 mA.

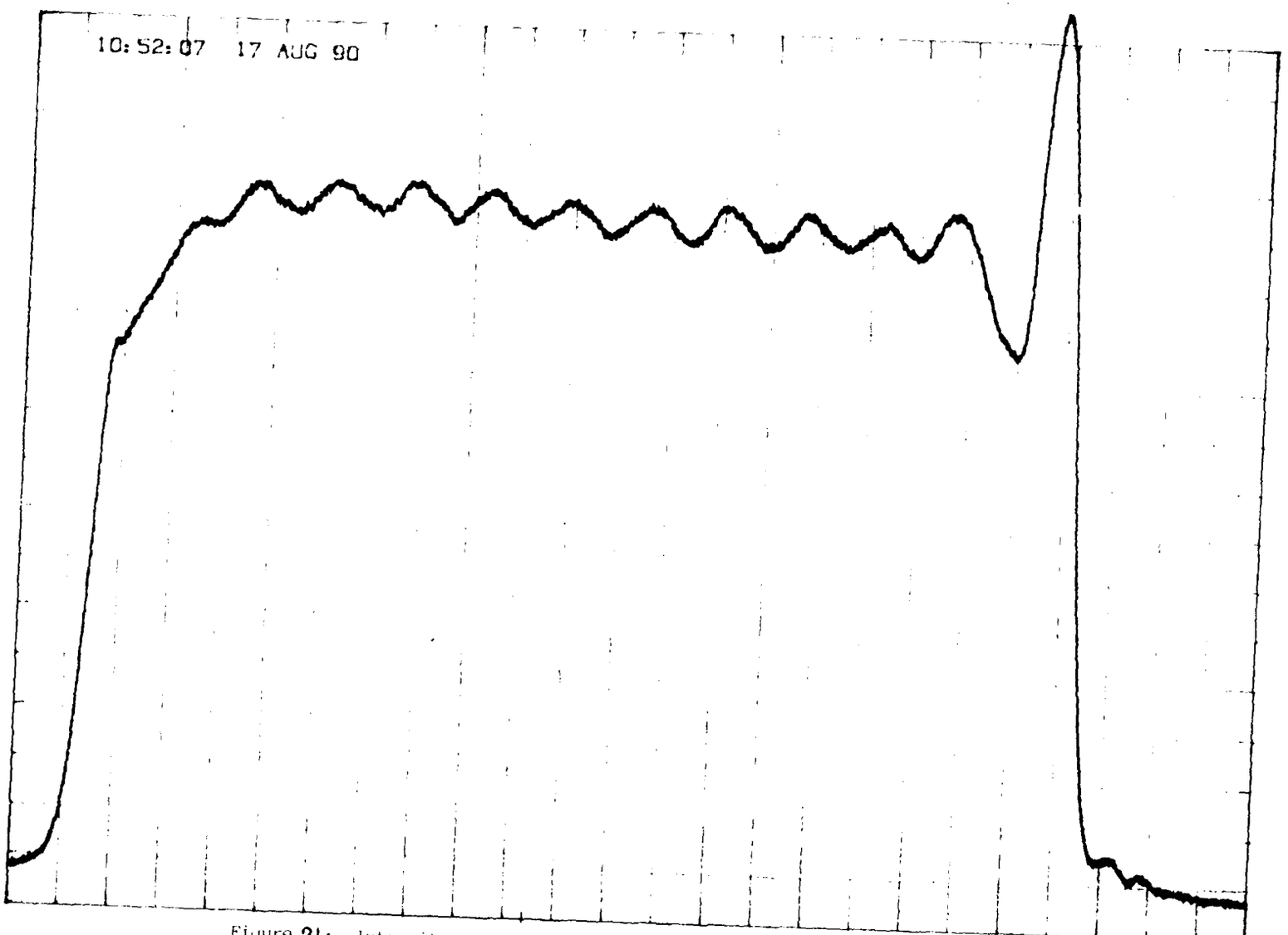

Figure 21: Intensity of Standing Striations in a Xenon Discharge for Discharge Currents of 18 mA.

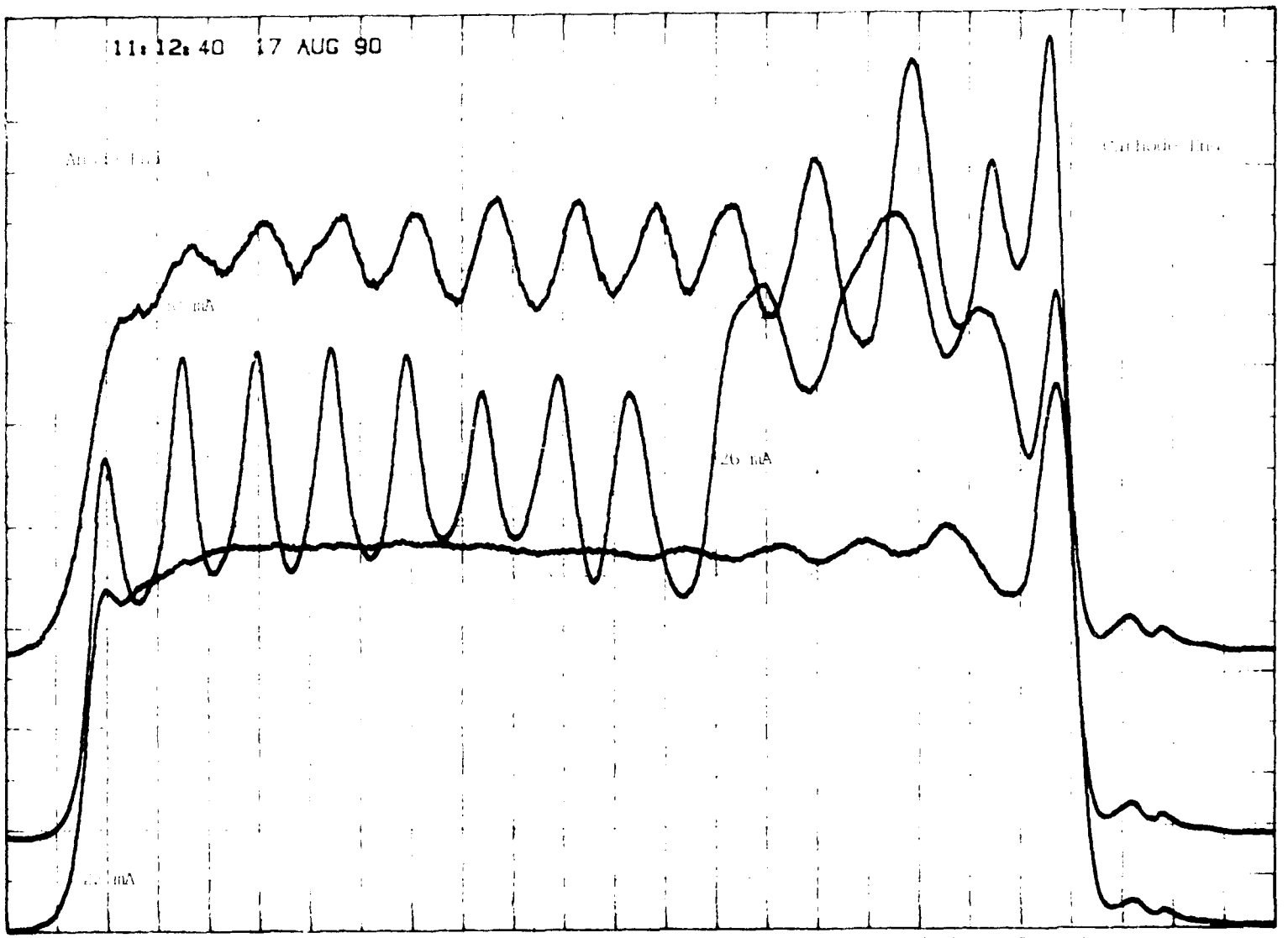

Figure 22: Intensity of Standing Striations in a Xenon Discharge for Discharge Currents of 22, 26, and 30 mA.

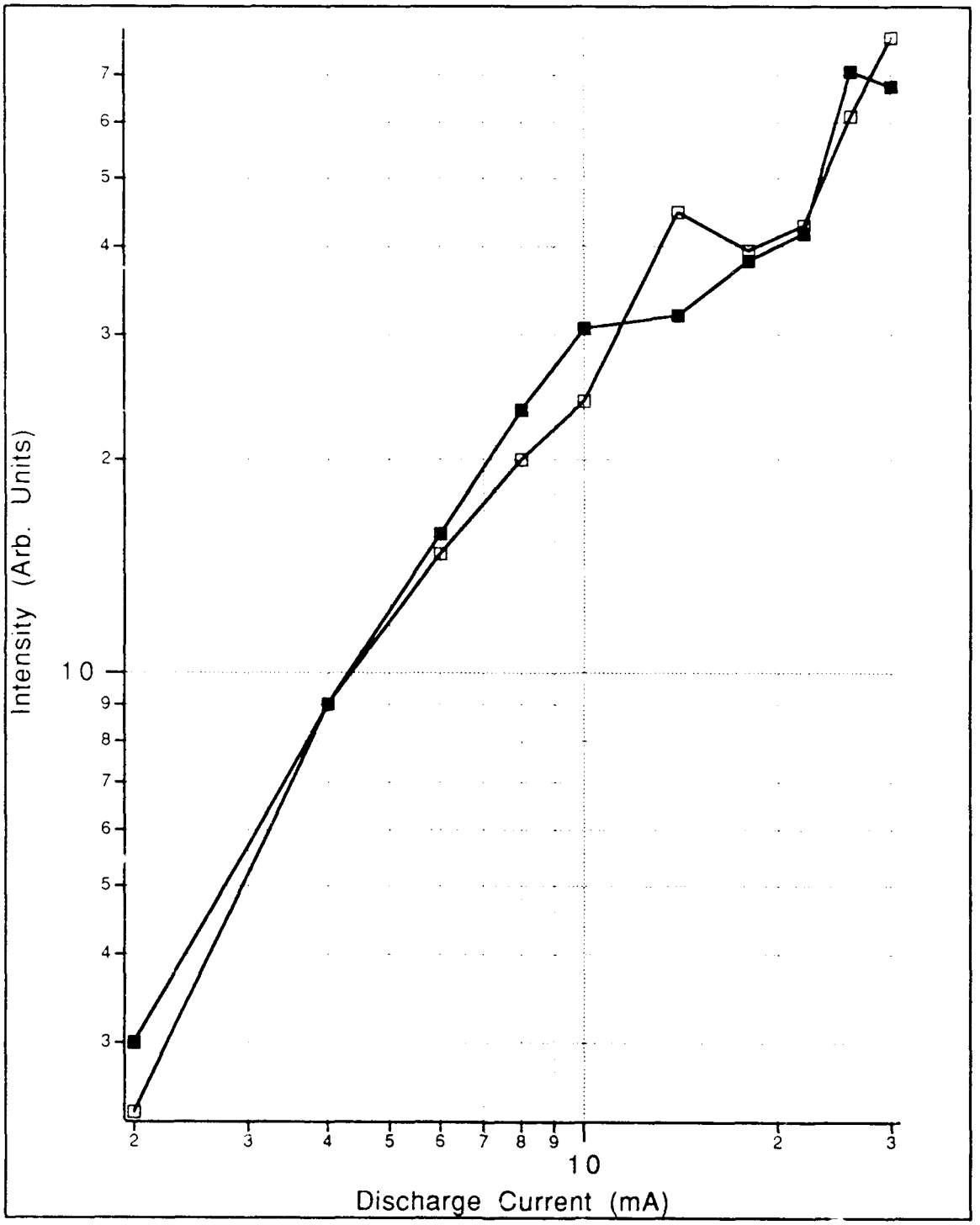

Figure 23: Variation in Intensity between Two Arbitrary Points separated by 4 cm along the Positive Column of a Xenon Discharge due to Standing Striations.

points chosen arbitrarily. For these two points the difference approached 20%.

In comparison with the conclusions of the striation theory discussed previously, the following trends were noted. First, the striations were severely damped for the 10 Torr case compared to the 1 Torr case. Second, the wavelength of the striations did not change between the two pressures, although this result is inconclusive since striations were resolvable at only one current setting at 10 Torr. These two results would tend to support the theory. On the other hand, damping towards the anode was not a consistent trend, although it was observed at some current settings.

Moving Striations . Moving striations were present in each tube regardless of the current, pressure, or radii considered. The intensity modulation typically approached 90%. The frequency of the oscillations was measured in the 10 Torr cold cathode tube and was typically ~ 1kHz. Generally, two dominant frequencies were observed, usually around 800 and 1800 Hz ± 200Hz. A map of moving striations with respect to PR and I/R is shown in figure 24. This range of occurrence is consistent with that of ref [ ].

The ratio of intensities for 7120Å, 7968Å , and 8409Å as a function of time for currents of 4 and 16 mA is shown in figures 25 and 26 respectively. Under equilibrium conditions, this ratio could be used to determine the excitation temperature modulation. However, it is unlikely that the excited state levels in a glow discharge are populated under thermal equilibrium conditions. On the other hand, if one assumes single step excitation of the

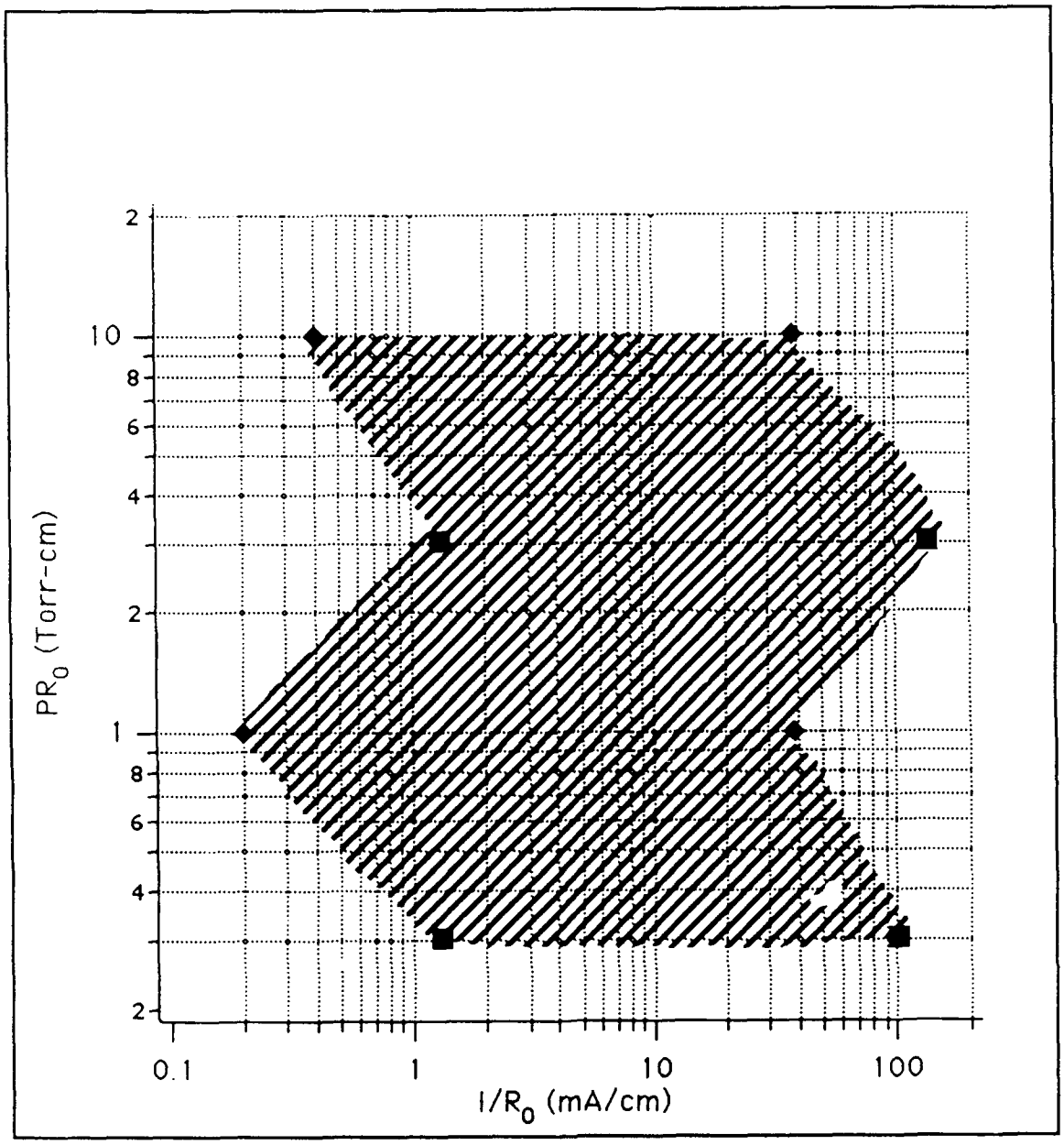

Figure 24: Map of Oscillation Regions for Xenon at 10 Torr, R = .3 cm

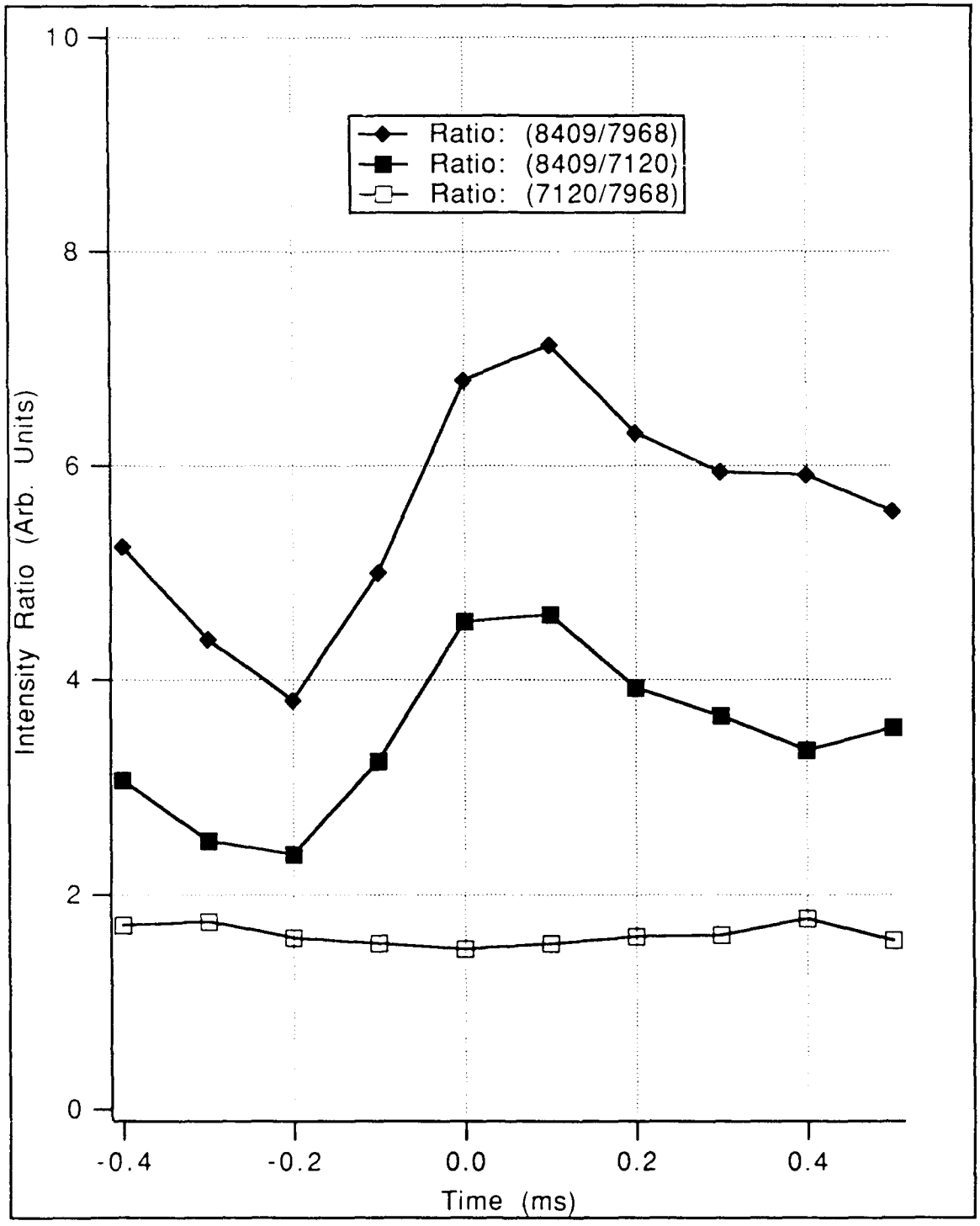

Figure 25: Intensity Ratio for Selected Transitions. Cold Cathode Tube @10 Torr 4 mA Discharge Current

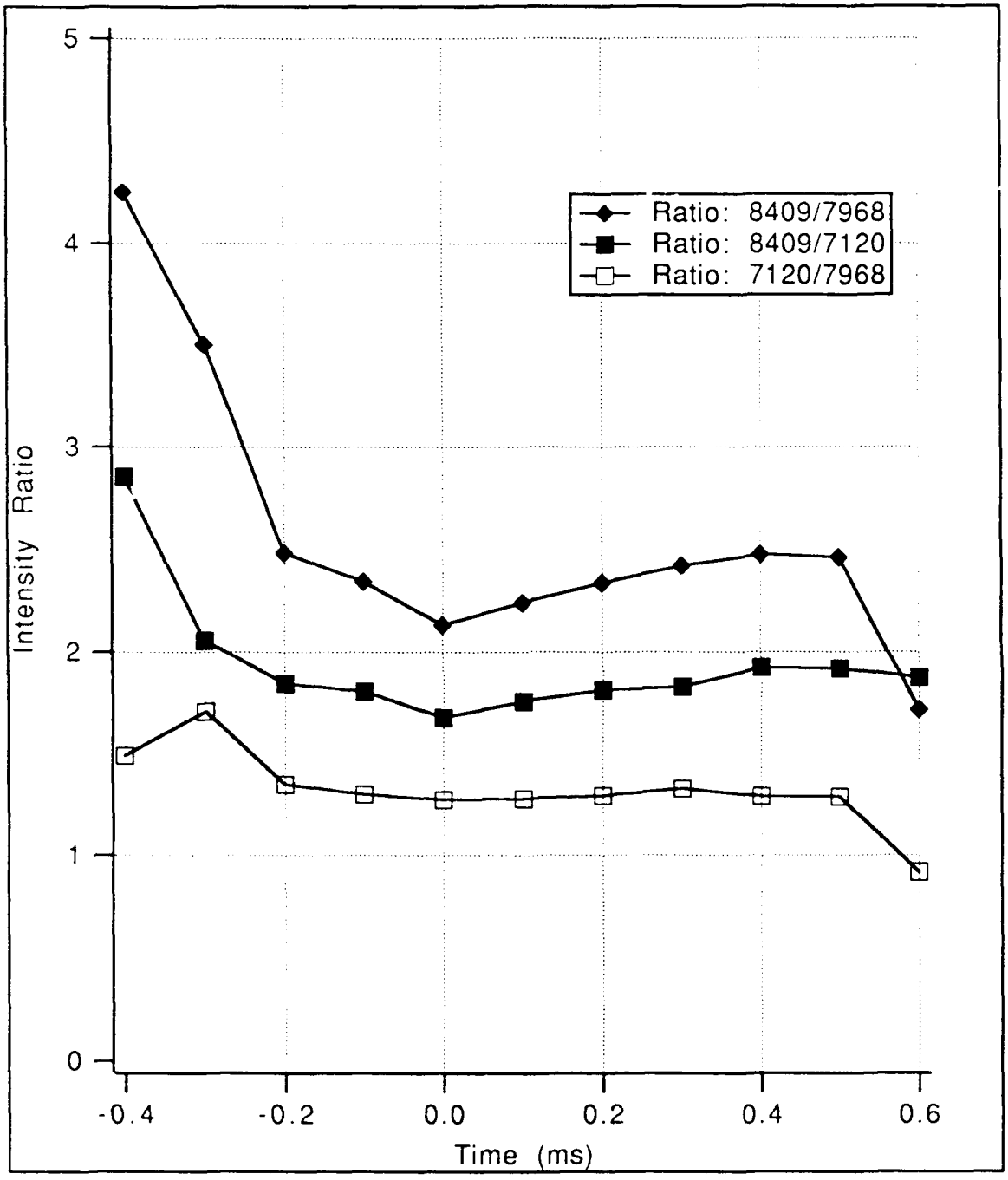

Figure 26: Intensity Ratio for Selected Transitions. Cold Cathode Tube at 10 Torr, 16 mA Discharge Current

excited state, and the electron energy distribution function is known, then this information shows the modulation of the effective excitation temperature. The intensity ratio of the 7p and 7d shows very little modulation for both cases. This could be due to their energy spacing being much smaller(~.5eV) than the others(~2eV).

It is not clear at this point how the oscillation characteristics compare to the theory for moving striations discussed in the background theory. Since one of the basic assumptions of the theory is that the plasma density perturbation is small, it may be that there is little correlation between the theory and the experiment because of the large modulation reported here. On the other hand, a quick calculation of the expected oscillation frequency based on the theory, assuming single step ionization and a Maxwellian EEDF, revealed that the expected oscillation frequency was about 2.5 to 3.4 kHz, for E_0 = 16 and 10 V, respectively. This is about a factor of two different than the measured frequencies.

Radiation Trapping . Unfortunately, measuring radiation trapping at the higher currents was abandoned because the tube used for this measurement has too wide a bore to get to higher densities without forming leaks. Nevertheless, radiation trapping was measured at 4 mA, which made for current densities of about 10^{11} cm^{-3}. It was assumed that , based on the discussion in the background section, that if radiation trapping were occurring, then the ratio of intensities would be different for the two discharge volume lengths. The measurement revealed that there was a

10% difference in the ratios, as shown in Table 1 below.

Table 1: Comparison of Intensity Ratios

RATIO	4624 / 7120	8409 / 4624	8409 / 7120
RADIAL (L=2cm	1.10	6.96	7.95
AXIAL L=30cm	1.20	6.70	8.24
% DIFF	9.1	-3.7	3.6

By comparison with Figure 7, the ratios would be expected to decrease for the axial measurements. The two cases shown in the table which would be expected to decrease the most actually increased. These variations may be due to the difference in geometry from that in the theory. The radial measurement is actually cylindrical rather than slab-like which may show a reduced intensity. In conclusion, it is expected that radiation trapping is not influencing the intensity measurements at the lower currents. It is not known whether or not radiation trapping is occurring at the higher currents, since it could not be measured. It is likely, however, to have a stronger influence at higher currents due to the increased population densities, brought about by higher currents.

VII. Conclusions and Recommendations

Conclusions . Due to the complicated inter-dependence of the metastable and excited states, the results of the voltage and intensity measurements are inconclusive as to whether single step or stepwise mechanisms are playing the dominant role. In summary, the decreasing voltage characteristic and the slight non-linear intensity trends seemed to indicate that stepwise mechanisms were operating in the hot filament tube at 1 Torr. The hot filament tube at 10 Torr showed contraction at about 4mA, in conjunction with a decreasing voltage characteristic, and a large sudden decrease in the intensity of the 8409Å line at 4-6mA. It is not clear why the voltage decreased by a factor of 7 over the current range, but the decrease in the intensity of the 8409Å line can be tied to the formation of Xenon molecular ions. The intensity of the other lines in this tube showed a linear current dependence. No clear indication of stepwise mechanisms occurred in the cold cathode discharge tube. The intensity varied linearly with current, and the increasing voltage characteristic The linear trends in the intensity are easily explained by single step excitation, but it seems likely to the author that stepwise mechanisms could also produce these trends under the right conditions. The trends observed in the voltage measurements could serve as an indicator of stepwise mechanisms, but could also be due to gas heating in the discharge.

Oscillations may be a serious factor in the accurate measurement and

interpretation in intensity measurements. It is not unreasonable to assume that some of the intensity trends observed at the lower pressures may be questionable since large variations in intensity were noted. In addition, this also leads one to question the intensity measurements reported by others, unless it is stated that the measurement was made for a homogeneous positive column.

Recommendations . Much work can still be done. First, since the estimations of the electric field dependence are questionable, the actual trends of the electric field in the discharge tubes is not known. It would be extremely useful to modify the tubes to include probes to measure the electric field accurately. On the other hand, the insertion of probes into the tubes could change the boundary conditions and possibly affect the operation of the discharge, in which case the relationship between the intensity of spectral lines of the probeless tubes of this experiment may not be applicable to the electric field measurements of the probed tube. A future topic may be the measurement of intensity and electric field in a probed tube, for comparison.

Secondly, the effects of gas heating are not clear in this experiment. Since the hot filament tube is fitted with a jacket for cooling, it may be useful to measure the difference between the tube with and withcut cooling.

Thirdly, an analytical examination of a four level system using available cross sections and distributions may also be useful. The author has already

begun such an endeavor, using linearized cross sections and maxwellian distributions. A refinement might be the use of a two temperature model to describe the electron energy distribution.

Fourth, since the system has been calibrated with respect to intensity vs wavelength for the various configurations(slit widths and heights, filters, etc), then the intensity measurements provide a means to determine the excitation temperature for all of the tubes, based on the various intensity ratio methods.

Appendix A

Comparison of average and peak intensity trends. The following figures show the comparison between the intensity trends observed on a DMM and an oscilloscope. Figure 27 is for the low currents while Figure 28 applies to the high currents. Vmax is the measured peak intensity of the waveform, while Vmin is the minimum value of the waveform. Vdiff represents the ratio between Vmax and Vmin, while Vave is the intensity recorded on the DMM. It appears from these results that the meter is actually reading close to the the minimum voltage of the waveform. This is probably due to the non-sinusoidal nature of the waveform, an example of which is shown in Figure 29. The ratio indicates that the measured intensity on the meter is probably an accurate representation of the intensity trends despite the oscillations, since this shows that both are increasing at the same rate.

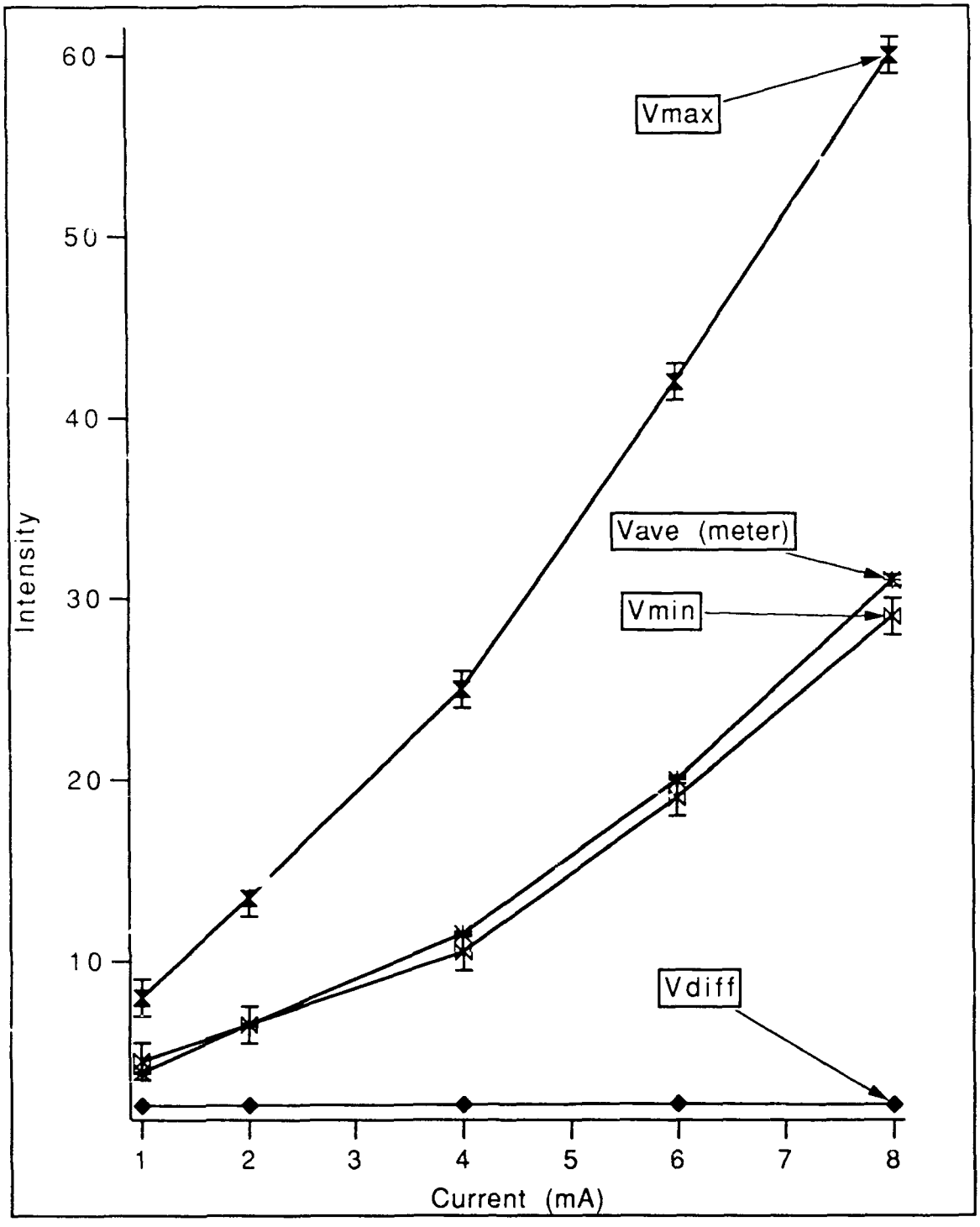

Figure 27: Intensity comparison between meter values and peak values, low currents

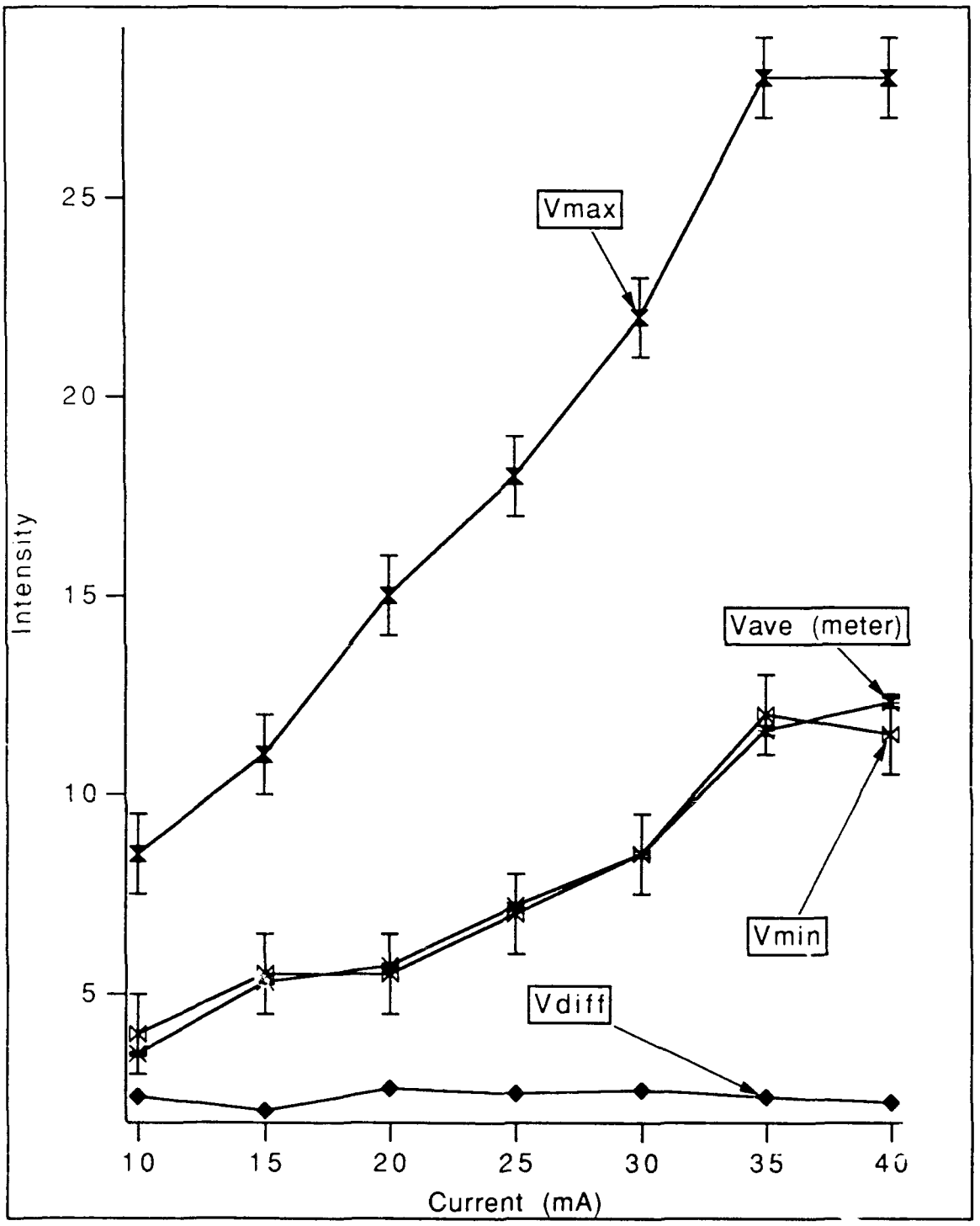

Figure 28: Comparison of Intensity Measurements between the DMM and the Oscilloscope. High Currents

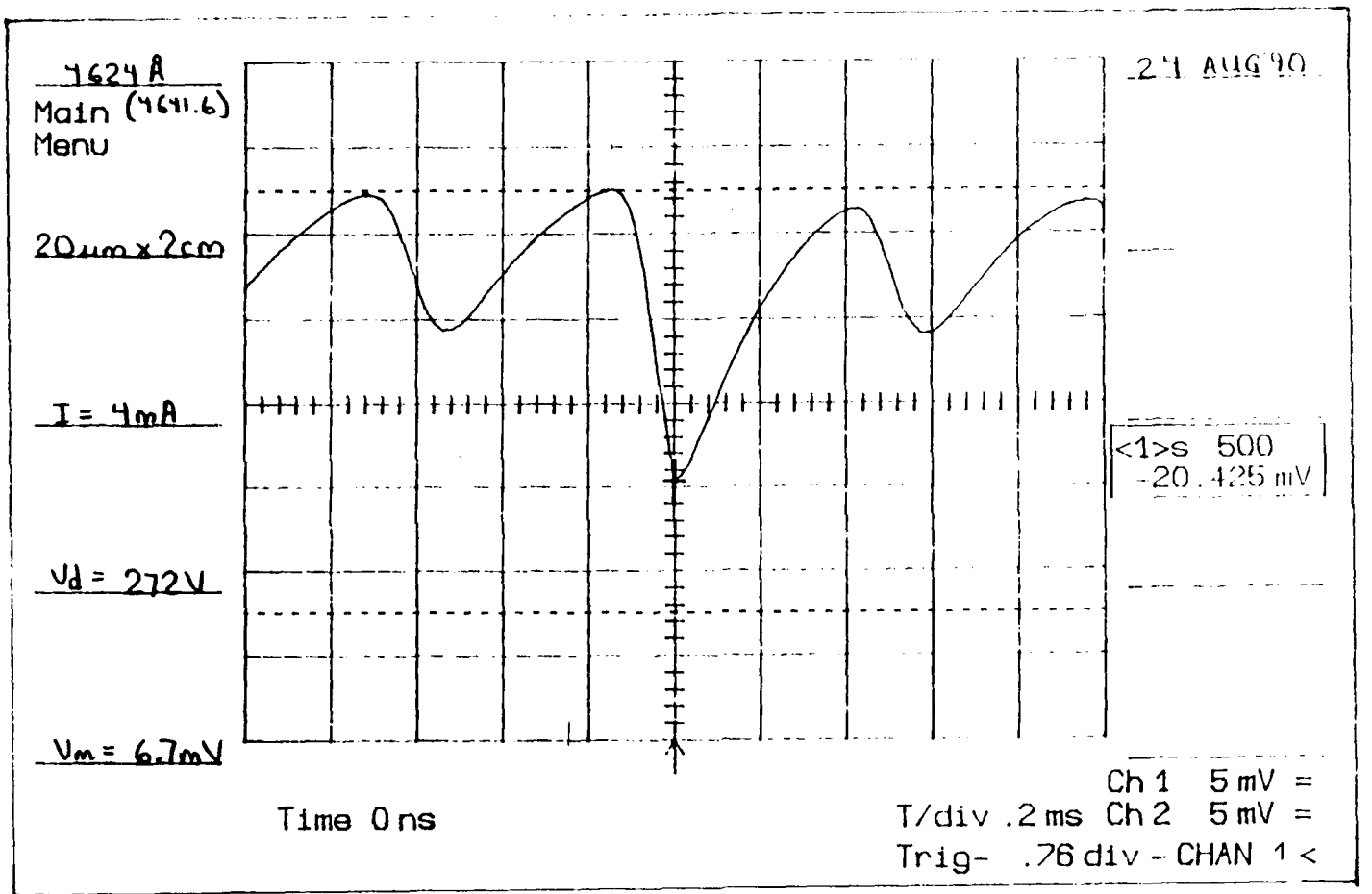

Figure 29: Example of Oscillation Waveform Measured

Bibliography

1. Glessner,J. W. Weapons Laboratory Tech. Report WL-TR-89-94

2. Plasma Class notes, AFIT,USAF

3. Barbetti, Beverini, and Sasso, Rev. Mod. Phys. **62** (3), 603(1990)

4. von Engel, A., p. 90

5. von Engel, p. 56-68

6. Bletzinger,P. Wright Research and development Center, Personal communication. Experimentally determined that in N_2, electrons in an electron beam lost about half of their energy to ionize the gas.

7. Cherrington, Gaseous Electronics and Gas Lasers

8. von Engel, A., p. 240

9. von Engel, A. p. 244

10. von Engel, A., p.248, fig 128, Although this fig is for Neon, it is assumed that the trends for Xenon will be approximately the same.

11. Mitchell, A., Zemanskii, M., *Resonance Radiation and Excited Atoms* , (University Press, Cambridge 1971)

12. DeJoseph, C., Wright Research and Development Center, personal communication, The author was unable to find written documentation on jl selection rules.

13. see, for example Herzberg, G., *Atomic Spectra and Atomic Structure* (Dover Pub., New York 1937)

14. Patrick, E. Wright State University, Dayton, OH, Personal communication work sponsored by WRDC, Wright Patterson AFB.

15. Garscadden, A., Gaseous Electronics, Vol 1, Chap 2.2 (Academic Press,1978)

16. Corney, A., *Atomic and Laser Spectroscopy,* (Clarendon Press, Oxford 1977)

17. Garscadden, A. Gaseous Electronics, Vol 1,Chap 2.2 (Academic Press,1978)

18. Francis, G, Encyclopedia of Physics,

19. Francis,G, *Ionization Phenomena in Gases* , (Academic,New York, 1960), p249 - 251

20. Pekarek, L., Czech. J. Phys. **B12**,450 (1962), **B13**, 881 (1963)

21. Lee, D. A., and Garscadden, A., J. Appl. Phys., **37**, 1, 377 (1966)

22.Lee, D. A., and Garscadden, A., Phys. Fluids., **15**, 10, 1826 (1972)

23. Brown, p.218, von Engel, p.223

24. Koruchkina, A., Sov. Phys. Tech. Phys., **20** (5) 676 (1976)

25. Kagan, Y., Lyagushchenko, R., and Khristov, N., Sov. Phys. Tech. Phys. **16** (10) 1627 (1972)

26. Brychkov, V., Eletskii, E., Sov. J. Plasma Phys., **4**, (4) 528 (1979)

27. Böwering, N., Bruce, M., Keto, J., J. Chem. Phys., **84** (2), 709 (1986)

Vita

Captain Ruark was born in Ypsilanti, Michigan. He enlisted in the United States Air Force in 1976, and worked as a Munitions Maintenance Specialist and Flight Simulator Specialist for the next 8 years. In 1983 he applied for and was accepted into the Air Forces Airman and Enlisted Commissioning Program, attending Michigan Technological University. Upon graduation with a BSEE, he endured a grueling period at Officer Training School and was commissioned 2nd Lieutenant in September 1986. Captain Ruark was then assigned to the Plasma Research Group at the Wright Research and Development Center, where he worked in the High Energy Densities Materials program for the next 2 years. He was assigned to AFIT in 1989.

REPORT DOCUMENTATION PAGE

Form Approved
OMB No 0704-0188

1. AGENCY USE ONLY (Leave blank)	2. REPORT DATE	3. REPORT TYPE AND DATES COVERED
	23 Nov 90	Final Thesis (Master's)

4. TITLE AND SUBTITLE
Operating Characteristics of Xenon Gas Discharges

5. FUNDING NUMBERS

6. AUTHOR(S)
Capt. Michael E. Ruark

7. PERFORMING ORGANIZATION NAME(S) AND ADDRESS(ES)
Air Force Institute of Technology
AFIT/ENP
Wright-Patterson AFB, OH 45433

8. PERFORMING ORGANIZATION REPORT NUMBER
AFIT/GEP/ENP/90D-06

9. SPONSORING/MONITORING AGENCY NAME(S) AND ADDRESS(ES)

10. SPONSORING/MONITORING AGENCY REPORT NUMBER

11. SUPPLEMENTARY NOTES

12a. DISTRIBUTION/AVAILABILITY STATEMENT
Approved for Public Release; Distribution unlimited

12b. DISTRIBUTION CODE

13. ABSTRACT (Maximum 200 words) Voltage-current and intensity-current characteristics were measured for four Xenon gas discharges. Four configurations consisting of a hot filament tube, and a cold cathode tube, were examined at 1 and 10 Torr. Intensity of the 8409Å, 4624Å, 7120Å, and 7968Å transitions, and discharge voltage were measured for each configuration for currents and pressures of .2 - 40 mA, and 1 and 10 Torr, respectively. Intensity dependence upon current was primarily linear in all cases with some important deviations, i.e. the hot filament tube at 10 Torr showed a large decrease in intensity between 4 and 6 mA in the 8409Å line. Voltage-current characteristic results were different for the different configurations. A decreasing characteristic was observed for a hot filament tube at both pressures, possibly due to the combination of gas heating and stepwise ionization. The voltage decreased in the hot filament tube at 10 Torr by a factor of seven over a current range of 1 to 40mA. Contsriction occurred in the hot filament tube at 10 Torr. Increasing voltage characteristics and abnormal cathode glow were observed in the cold cathode tube at both pressures. both spatial and temporal instabilities were observed in all cases. Temporal modulation approached 90% while spatial modulation approached 30%.

14. SUBJECT TERMS	15. NUMBER OF PAGES
Xenon, Gas Discharges, Operating Characteristics, Oscillations	100
	16. PRICE CODE

17. SECURITY CLASSIFICATION OF REPORT	18. SECURITY CLASSIFICATION OF THIS PAGE	19. SECURITY CLASSIFICATION OF ABSTRACT	20. LIMITATION OF ABSTRACT
Unclassified	Unclassified	Unclassified	UL

REPORT DOCUMENTATION PAGE

Form Approved
OMB No. 0704-0188

1. AGENCY USE ONLY (Leave blank)	2. REPORT DATE	3. REPORT TYPE AND DATES COVERED
	Dec 90	Master's Thesis

4. TITLE AND SUBTITLE

Operating Characteristics of Xenon Gas Discharges

5. FUNDING NUMBERS

6. AUTHOR(S)

Michael E. Ruark, Captain, USAF

7. PERFORMING ORGANIZATION NAME(S) AND ADDRESS(ES)

Air Force Institute of Technology
WPAFB, OH 45433-6583

8. PERFORMING ORGANIZATION REPORT NUMBER

AFIT/GEP/ENP/90D-06

9. SPONSORING/MONITORING AGENCY NAME(S) AND ADDRESS(ES)

10. SPONSORING/MONITORING AGENCY REPORT NUMBER

11. SUPPLEMENTARY NOTES

12a. DISTRIBUTION/AVAILABILITY STATEMENT

Approved for public release, distribution unlimited

12b. DISTRIBUTION CODE

13. ABSTRACT *(Maximum 200 words)*

Voltage-current and intensity-current characteristics were measured for four Xenon gas discharges. Four configurations consisting of a hot filament tube, and a cold cathode tube, were examined at 1 and 10 Torr. Intensity of the 8409Å, 4624Å, 7120Å, and 7968Å transitions, and discharge voltage were measured for each configuration for currents and pressures of .2 - 40 mA, and 1 and 10 Torr, respectively. Intensity dependence upon current was primarily linear in all cases with some important deviations, i.e. the hot filament tube at 10 Torr showed a large decrease in intensity between 4 and 6 mA in the 8409Å line. Voltage-current characteristic results were different for the different configurations. A decreasing characteristic was observed for a hot filament tube at both pressures, possibly due to the combination of gas heating and stepwise ionization. The voltage decreased in the hot filament tube at 10 Torr by a factor of seven over a current range of 1 to 40mA. Contsriction occurred in the hot filament tube at 10 Torr. Increasing voltage characteristics and abnormal cathode glow were observed in the cold cathode tube at both pressures. both spatial and temporal instabilities were observed in all cases. Temporal modulation approached 90% while spatial modulation approached 30%.

14. SUBJECT TERMS	15. NUMBER OF PAGES
Xenon, Gas Discharge, Low Pressure, Lasers, Oscillations	100
	16. PRICE CODE

17. SECURITY CLASSIFICATION OF REPORT	18. SECURITY CLASSIFICATION OF THIS PAGE	19. SECURITY CLASSIFICATION OF ABSTRACT	20. LIMITATION OF ABSTRACT
Unclassified	Unclassified	Unclassified	UL